



POLITECNICO DI TORINO  
Repository ISTITUZIONALE

Study, development and characterization of aluminum based materials by additive manufacturing

*Original*

Study, development and characterization of aluminum based materials by additive manufacturing / Canali, Riccardo. - (2015).

*Availability:*

This version is available at: 11583/2598770 since:

*Publisher:*

Politecnico di Torino

*Published*

DOI:10.6092/polito/porto/2598770

*Terms of use:*

openAccess

This article is made available under terms and conditions as specified in the corresponding bibliographic description in the repository

*Publisher copyright*

(Article begins on next page)

# POLITECNICO DI TORINO

PhD School in Materials Science and Technology

PhD Thesis

**Study, development and characterization of aluminum  
based materials by additive manufacturing**



Riccardo Canali

**Academic Supervisor**  
Prof. Paolo Fino

**PhD Program Coordinator**  
Prof. Claudio Badini

XXVII Cycle 2012-2014

Academic Year 2014 - 2015

# Contents

<b>I</b>	<b>Theory and methods</b>	<b>4</b>
<b>1</b>	<b>Introduction</b>	<b>5</b>
<b>2</b>	<b>Additive Manufacturing insights</b>	<b>8</b>
2.1	Recent technological advances . . . . .	8
2.2	Additive Manufacturing/3D printing . . . . .	14
2.2.1	Stereolithography (STL) . . . . .	16
2.2.2	Fused Deposition Modeling (FDM) . . . . .	17
2.2.3	Examples of materials for AM/3D printing . . . . .	17
<b>3</b>	<b>Additive Manufacturing for metals</b>	<b>19</b>
3.1	AM technologies for metallic materials . . . . .	19
3.1.1	Electron Beam Melting (EBM) . . . . .	22
3.1.2	Laser Engineered Net Shaping (LENS) . . . . .	24
3.1.3	Selective laser sintering (SLS) . . . . .	26
3.2	Selective Laser Melting (SLM) . . . . .	28
3.2.1	Mechanisms involved . . . . .	28
3.2.2	Microstructural properties after SLM . . . . .	32
3.2.3	Main SLM parameters . . . . .	39
3.2.4	Systems and manufacturers . . . . .	41
3.2.5	SLM for Metal Matrix Metal Composites (MMCs) production . . . . .	42
<b>4</b>	<b>Methods and characterizations</b>	<b>45</b>
4.1	DMLS . . . . .	45
4.1.1	EOSINT M270 Xtended machine . . . . .	45
4.2	Characterization methods . . . . .	49
4.2.1	Density and porosity evaluation methods . . . . .	49
4.2.2	Mechanical characterization . . . . .	52
4.2.3	Field Emission Scanning Electron Microscope (FESEM) . . . . .	53
4.2.4	X-ray diffraction (XRD) . . . . .	53
4.2.5	Nanohardness and Scanning Probe Microscopy (SPM) . . . . .	54

<b>II</b>	<b>Experimental activities</b>	<b>59</b>
<b>5</b>	<b>Results and discussion</b>	<b>60</b>
5.1	AlSi10Mg by DMLS . . . . .	60
5.1.1	“Process window” of AlSi10Mg alloy: density optimization	61
5.1.2	Powder characterization . . . . .	63
5.1.3	Mechanical properties evaluation . . . . .	66
5.1.4	Microstructural characterization . . . . .	72
5.1.5	Heat treatment: T6 cycle characterization . . . . .	78
5.2	AlSi10Mg/SiC (10% in wt.) composite . . . . .	81
5.2.1	Starting material . . . . .	82
5.2.2	Density and porosity evaluation . . . . .	86
5.2.3	Mechanical properties evaluation . . . . .	94
5.2.4	Nanohardness characterization . . . . .	95
5.2.5	Microstructural characterization . . . . .	98
5.3	AlSi10Mg/nanoMgAl <sub>2</sub> O <sub>4</sub> (0.5% in wt.) composite . . . . .	103
5.3.1	Starting material . . . . .	103
5.3.2	Density and porosity evaluation . . . . .	104
5.3.3	Microstructural characterization . . . . .	106
<b>6</b>	<b>Conclusions</b>	<b>108</b>
<b>7</b>	<b>Bibliography</b>	<b>110</b>

## Part I

# Theory and methods

# Chapter 1

## Introduction

The manufacturing industry is always looking for ways to improve production while reducing cost. Traditional material subtractive manufacturing technologies such as, milling, tapping, turning, etc. create 3D physical models by removing material using cutting tools. The movement of the cutting tools is manually controlled by the machinist. With the rapid development of CAD/CAE technology since early 1970s, automated manufacturing processes with numerical control machine tools have become possible. The emergence of Computerized Numerical Control (CNC) and High Speed (HS) milling technologies reduce the process time and hence significantly increase the productivity. However, as a mature technology, subtractive manufacturing still has some disadvantages due to its working principle. One major disadvantage is the dependence on the geometric complexity. Features such as small holes inside a block are hard to manufacture due to the process constraints, i.e. the interference between the cutting tool and part. Additionally when the sample size is small, the time for process planning and CNC programming can constitute a significant portion of the time required to manufacture the part.

Unlike traditional subtractive machining processes, Rapid Prototyping (RP) (also termed as Layered manufacturing (LM) or Solid Freeform Fabrication (SFF)) is a material additive manufacturing process. In a product development context, the term Rapid Prototyping (RP) was widely used to describe technologies which created physical prototypes directly from digital data. The first methods for rapid prototyping became available in the late 1980s and were used to produce models and prototype parts. Users of RP technology have come to realize that this term is inadequate to describe the more recent applications of these technologies. The ASTM F-42 committee was recently formed to standardize Additive Manufacturing (AM) terminology and develop industry standards. According to their first standard, ASTM F2792-10, AM is defined as “The process of joining materials to make objects from 3D model data, usually layer upon layer, as opposed to subtractive manufacturing technologies”. The basic principle of this technology is that a geometric model, initially generated using three-dimensional Computer Aided Design (3D CAD) system (e.g. Solid-

Works), can be manufactured directly without the need of process planning. There are many related terms used to describe AM and common synonyms include: additive fabrication, additive layer manufacturing, direct digital manufacturing, 3D printing and freeform fabrication. Within the last 20 years, AM has evolved from simple 3D printers used for rapid prototyping in non-structural resins to sophisticated rapid manufacturing systems that can be used to create functional parts in different engineering materials directly without the use of tooling. Most work to date has been conducted using polymer materials, but the development of AM processes such as Selective Laser Sintering/Melting, Electron Beam Melting and Laser Engineered Net Shaping enabled to build parts by using metallic materials, metal matrix composites and ceramic materials. Additive manufactured parts are now utilized in aerospace, automotive, medical fields and also in consumer products and military. Additive manufacturing or 3D printing is receiving unprecedented attention from the mainstream media, investment community, and national governments around the world. Prototyping has been the technology's biggest application, thus the name rapid prototyping, and it remains a key category. The fastest-growing application, however, is in the actual manufacturing of parts for final products. In just 10 years, this important application has grown from almost nothing to more than 28% of the total global product and service revenues. The manufacturing of final parts, rather than prototyping, is where the manufacturing money is, and it is the most significant part of AM's future. Researchers and industry leaders in the European Union (EU) have identified AM as a key emerging technology. Teaming relationships have been formed between university, industry, and government entities within and across countries. Large aerospace companies, such as Boeing, GE Aviation, and Airbus, are hard at work qualifying AM processes and materials for flight. Boeing, for example, now has 200 different AM part numbers on 10 production platforms, including both military and commercial jets.

### Objective of the research

Direct Metal Laser Sintering (DMLS), trademark of EOS to indicate SLM, is a particular Additive Manufacturing technique for the fabrication of metallic and composites near net-shaped parts directly from CAD through the melting of successive thin layers of powder (30  $\mu\text{m}$ ) due to a laser source. Its application for manufacturing 3D objects with complex geometries or lattice structures represents one of the most promising directions to solve challenging industrial problems (i.e. in the aerospace field). Many materials have been processed successfully and many works are available in the literature on the DMLS of iron and steels, superalloys, titanium and aluminum alloys.

This PhD thesis work was pursued in a context of investigation and development of different kind of materials by DMLS, in particular aluminum alloys. Among these, AlSi10Mg0.3 casting alloy was investigated and characterized from both mechanical and microstructural (through optical and electron microscopy) point of view. It was previously fundamental to study the process parameters (in particular scan speed, laser power and hatching distance) in order to obtain samples with density near to the theoretical one for the different characterizations.

In addition, processing of composite materials has attracted interest due to the potential of the process in freeform fabrication of intricate articles in a reduced supply chain. For this reason, the studied alloy was used as a matrix to fabricate two different “ex-situ” Aluminum Matrix Composites (AMCs): starting from AlSi10Mg powders and mixing them with submicrometric SiC and nanometric  $\text{MgAl}_2\text{O}_4$ . It was fundamental to investigate the effect of the main process parameters to obtain composites with the highest density, to be then characterized.

### Thesis outline

The PhD thesis is organized as follows:

- chapter 2 is a literature review on the research work related to AM processes, including 3D printing for polymeric materials;
- chapter 3 introduces and emphasises the processes suitable for metallic materials, in particular DMLS;
- chapter 4 is divided in two sections: the first presents the DMLS specific machine, including its build strategies, and the second one shows the characterization methods which were adopted in the experimental activities;
- chapter 5 illustrates the experimental results obtained by characterizing the fabricated alloy and the derived composites;



## Chapter 2

# Additive Manufacturing insights

### 2.1 Recent technological advances

The present chapter contains a global overview of Additive Manufacturing technologies, its most recent developments and improvements. These are pushed by both an increasing number of companies and research institutes too, involved in a world where it is really clear that the satisfaction level of the individual customer is exponentially increasing. More and more entrepreneurs either have adopted or are most likely going to adopt this technological approach, which is in general based on the addition of material layer by layer to build objects, opposite to the material removal from a bulk. First of all this fact arised to satisfy the increasing demand of customized goods, and this fact reflects upon the AM level of spread. According to the work published by Wohler T. and Associates, the number of AM machines sold all around the world has no more stopped increasing for the past ten to fifteen years [1]. This annual report represents a reference point not only for the many research groups focused on AM but also for the industrial adopters. AM spread goes back to the late 80's, with a quite definite breakthrough point in the middle 90's, as the reader can clearly see in figure 2.1. The pie chart which is reported shows the results of a survey in 2013 concerning the percentages of gain of worldwide AM providers divided by single industrial sectors.

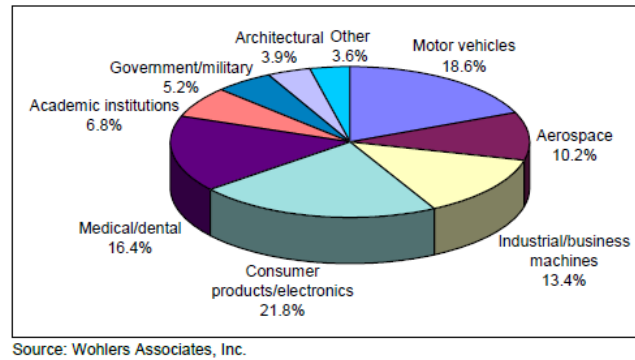


Figure 2.1: Courtesy of Wohler's Associates, Inc. [1]

The global market AM products and services grew 29% (compound annual growth rate) in 2012 to over \$ 2 billion. Unit sales of professional-grade, industrial systems reached nearly 8,000 units in 2012 (excluding the sales of personal 3D printers that sell for under \$ 5,000). This is an increase from an estimated 6,500 units in 2013 and demonstrates a growth trend of industrial AM systems sales worldwide: figure 2.2 would help to have a quantitative idea of the growing trend.

**AM and 3D printing industry (products and services) worldwide projected value**

2015	\$4 billion
2017	\$6 billion
2021	\$10.8 billion

Figure 2.2: Data from Wohler's Report 2013 [1]

Significantly faster, the global growth of personal 3D printers averaged 345% each year from 2008 to 2011. In 2012, interestingly, the increase was estimated at only 46.3%. Most of these machines are being sold to hobbyists, do-it-yourselfers, engineering students, and educational institutions. The use of AM for the production of parts for final products continues to grow in a constant way. In ten years it has gone from almost nothing to 28.3% of the total product and services revenue from AM worldwide. Within AM for industry, there has been a greater increase in direct part production, as opposed to prototyping, which represented the AM traditional area of dominance in its early stage. Within direct part production, AM serves a wide list of products and sectors including consumer electronics, textiles and fabrics, film effects, jewellery and musical instruments.

Three of the fastest growing areas for AM include the medical and dental, automotive and aerospace sectors. The success of AM in the biomedical sector consists of its ability to create customised prosthetics, implants, replacement tissues and intricate body parts, including for example blood vessels. The largest adopter has been the aerospace industry with the entrance of in particular metals fed AM machines into the industry in 2011, resulting in good take up of the technology owing to advantages of speed, cost and materials use rationalisation. For example, in the case of metallic powder bed processes, it is possible to recycle the not “consumed” powders and this strongly contributes to reduce the environmental impact if you take into account the supply chain. On the contrary, subtractive technologies generally produce a significant amount of waste material, i.e. the machining scraps. The graph in figure 2.3 shows the evolution of AM in time.

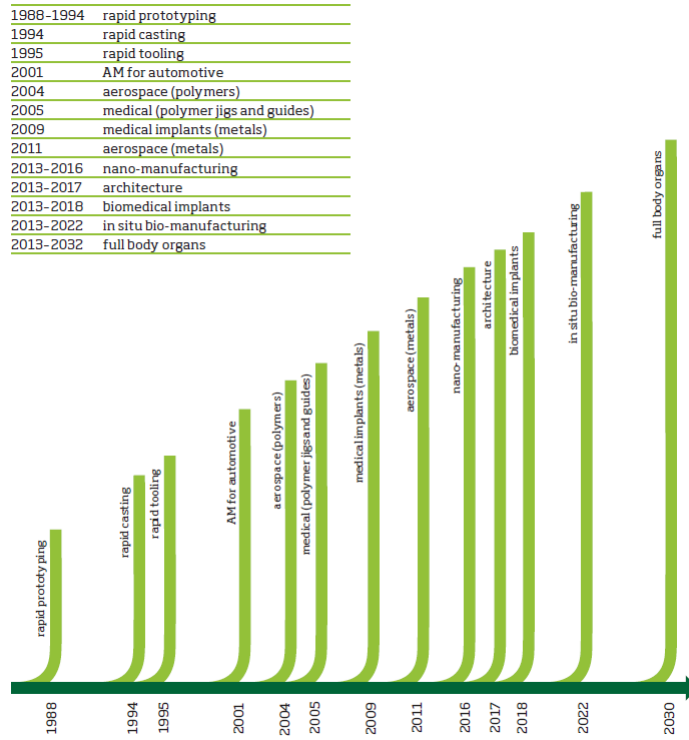


Figure 2.3: AM applications timeline [2]

Considering the supply chain, there is also a lead time benefit for the raw material acquisition. For example, large billets of titanium need to be ordered one or two years before they are used. However, the same material in powder form can often be purchased immediately.

For low-volume production, AM offers faster lead times than traditional manufacturing methods. For example, in Formula One racing competitions, engineers are using AM to manufacture parts in a highly reactive way. “They can now analyse the car’s performance while it goes round the circuit and have a new part getting ready before it finishes the race,” was reported by Graham Tromans, principal and president of AM consultancy GP Tromans Associates [2]. Rolls-Royce is verging on using AM to manufacture entire components. Moreover, AM has the capability to simplify and shorten the manufacturing supply chain. Another important aspect is the possibility to build objects in one piece with movable parts: it means that there are savings in assembly and maintenance. An example of a final use component is given in figure 2.4.

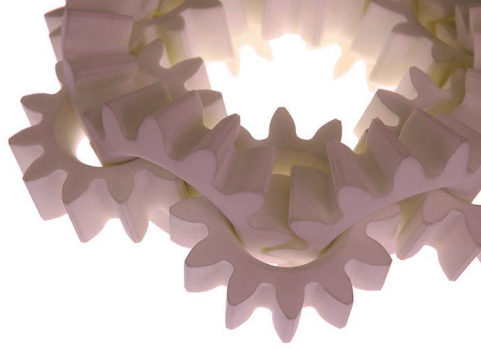


Figure 2.4: A sample component realized by Rolls-Royce [2]

To make the most of the potential of AM techniques, designers have to adapt their approach to these technologies, and some limitations arise. In fact, it is required to move away from the idea of replicating what is already built in other ways by other kind of technologies, i.e. by CNCs. Some examples of unimaginable objects to be realized in a single-step philosophy without the possibilities offered by AM are illustrated in figure 2.5.

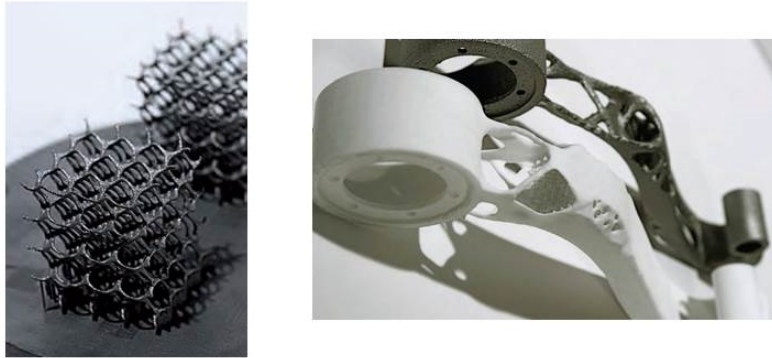


Figure 2.5: Examples of objects obtained by AM technologies: a metallic lattice (on the left) and an assembly (on the right) [2]

Despite its clear benefits, AM remains beset by some technological issues and suffered at the beginning from the lack of a supportive framework, underfunding and a lack of industry standards. First of all, data are the language without which AM would not function. While AM technologies have been in existence for around 25 years, it is data management which is the new aspect of the technology, with the potential to accelerate uptake of AM. In addition, whereas low-volume production is faster than conventional manufacturing, higher volumes are still considerably slower. It is also difficult for AM technologies to compete with traditional techniques on reliability and reproducibility of the final outputs.

AM is an umbrella term given to the whole set of technologies which guarantee the manufacturing of parts by adding material in a layer upon layer approach, as opposed to the so called conventional technologies, which are instead subtractive, in which the material is removed from an original bulk through a step by step subsequent machining operations. The ASTM F - 42 committee was recently formed to standardize AM terminology and develop industrial standards, and this is another significant proof of the increasing impact of these technologies. According to their first standard, ASTM F2792 - 10, AM is defined as “The process of joining materials to make objects from 3D model data, usually layer upon layer, as opposed to subtractive manufacturing technologies”. The basic principle of this technology is that a geometric model, initially generated using a three - dimensional Computer Aided Design (3D CAD) system (i.e. CATIA, Pro/Engineer, Solid Works), can be manufactured directly without the need of a specific process planning [3].

Nowadays, a clear distinction is made between Rapid Prototyping , RP, and Rapid Manufacturing, RM, as reported by many authors. Kruth J.-P. and his research group in Leuven concisely proposed the following [4]:

- **RP** refers to the realization of prototypes, visual design aids, fit and assembly test parts, mainly functional, in a product development phase as

support tools, which are not expected to be equivalent to the real produced parts at all levels and applications. RP was the initial widely accepted term used to refer to all layer additive manufacturing processes, since the synergistic combination of materials and processes was not sufficiently advanced to allow functional applications.

- **RM** means the direct production of fully functional parts (final products to be used directly), and should fulfill all the requirements and specifications required to such components. In detail, Rapid Tooling (RT) can be considered in this context, in particular in terms of production of different kind of tool objects.

AM technologies produce parts through the polymerization, fusing or sintering of materials in form of predetermined layers. By AM means, you enable the direct realization of geometries which are almost impossible to produce using other machining or moulding processes. The processes do not require predetermined tool paths. Features like draft angles or undercuts and internal channels can be designed and more easily obtained. As published in previous studies in the research group in which this PhD thesis was pursued [3,5], a new free-form design approach is possible by adopting AM. As examples, a couple of trabecular structures in Al alloy are shown in figure 2.6.

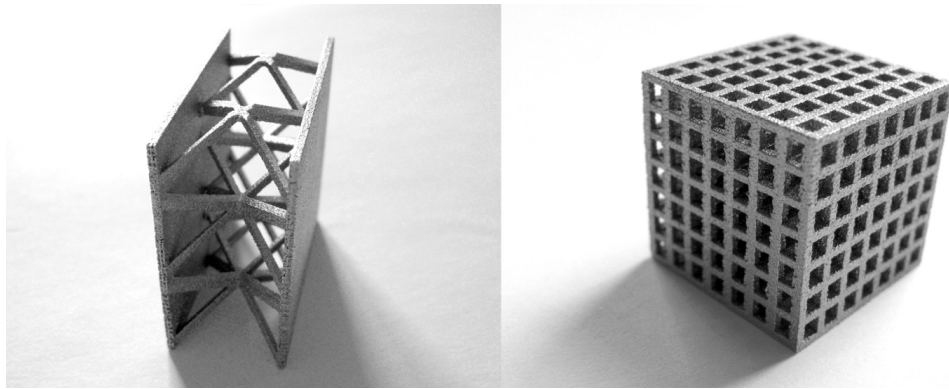


Figure 2.6: Trabecular structures realized in aluminium by SLM/DMLS [3]

The layers of all AM parts are generated by slicing a set of CAD data, by the use of a specialist software. The whole series of AM technologies work applying this principle. However, the thickness of the layer is one of the main parameters dependent on the considered system. Its typical range available in commercial systems is from 16 up to 200 micrometers. In some cases, the layers are visible on the surface of the part, influencing the surface final quality. This is known as the staircase effect and it has a relationship with the layer thickness and the

orientation of a surface. The thinner each layer is and the more vertical the orientation of a part wall, the smaller each step will be, resulting in a smoother surface quality. The thinner the layer is, the longer the processing time and the higher the final part resolution. Successive layers are built up one on top of the previous one along the direction generally indicated by z axis. After processing a single layer, a new layer of material is deposited, by using many different ways. For example, with polymeric resin based systems, the parts submerge in the resin by one layer thickness along the building direction and a traversing edge flattens the resin before the material processing. With powder bed systems, powder is deposited and spread using a recoating system. Since time of processing can be interpreted in terms of energy sources consumption, the most efficient way to produce parts via AM is to build many parts simultaneously. For this reason, many softwares have been developed to orientate properly and position the multiple parts within a virtual representation of the AM system.

## 2.2 Additive Manufacturing/3D printing

In general, AM technologies could be categorised in different ways. Kruth et al. [4] proposed the scheme reported in Table 2.1 to summarize the main aspects concerning the most common AM technologies:

Technique	Layer creation technique	Phase Change during layer solidification	Materials
Stereolithography (SLA)	Liquid layer deposition.	Photo-polymerisation.	Photo-polymers e.g. acrylates, epoxies, filled resins (glass, ceramic, metal) and colourable resins.
Laminated Object Manufacturing (LOM)	Deposition of sheet metal.	No phase change.	Paper, polymer, polymer foam, composites, ceramics and metals.
Fused Deposition Modelling (FDM)	Continuous extrusion and deposition.	Solidification by cooling.	Polymers, wax, filled polymers, metals with binders, ceramic with binders.
Selective Laser Sintering (SLS)	Layer of powder	Laser sintering / laser melting and re-solidification by cooling.	Polymers, metals with binders, pure metals, sand and ceramics.
3D Printing (3DP)	Layer of powder + Drop-on-demand binder printing.	No phase change.	Ceramic with binder, polymer with binder, and metals with binder.

Table 2.1: Summary of the most common AM technologies [4]



### 2.2.1 Stereolithography (STL)

Stereo Lithography Apparatus is the first commercialized AM process. Stereo Lithography Apparatus works by curing photosensitive resin with the aid of UV laser layer upon layer to produce a 3D part. Photo curable resins such as epoxy, vinyl ether or acrylate are used. Figure 2.7 shows the schematic of Stereo Lithography Apparatus. Based on the CAD data, Laser beam cures a selected portion of a vat of resin and the resin is solidified on a platform. The laser light moves in x/y plane to cure the resin. Then the platform is moved down to the height of one layer. Then the next layer of liquid resin is deposited by the sweeper and cured by the laser beam. The process is repeated until part building is finished. Support structures are needed for the overhanging parts. They are removed after the part building and post processing is done under UV light or thermal oven to cure the uncured resin [6], [7]. Stereo Lithography Apparatus is marketed by 3D systems (USA).

Polyjet process is another important commercialized process, which belongs to jetting systems. Objet developed the Polyjet process and this process was marketed through Objet Quadra machine in 2000. Polyjet process utilizes an array of printing heads to selectively deposit the acrylate based photopolymer. Support material is deposited by using second series of printing heads. An UV lamp is used to cure the photopolymer by passing over the deposited material. The layer thickness is usually 16  $\mu\text{m}$  [6].

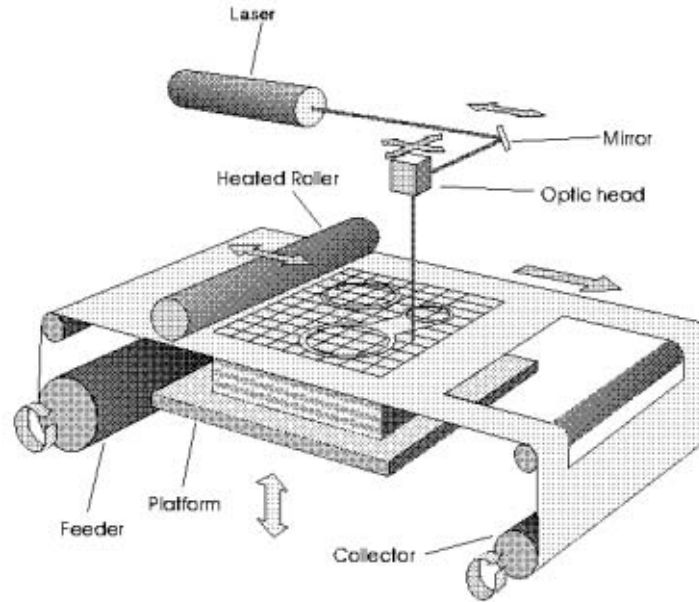


Figure 2.7: Stereolithography working principle (STL) [6]

Polymer powder flowability could be increased by adding some powder (around 1  $\mu\text{m}$  size) of glassy oxide, hydrated silica, fluoro plastics, and metallic stearates, but it needs to be ascertained whether these additions change final properties significantly [8].

### 2.2.2 Fused Deposition Modeling (FDM)

AM Processes which produce a 3D part by using a solid raw material belong to another category. The most known technology, which parts are produced by extruding material through a nozzle, is Fused Deposition Modelling (FDM). The nozzle moves in the x/y plane to build up a layer. The FDM process typically utilizes thermoplastic material to produce parts. A different material is used for supports. Figure 2.8 depicts the schematic of FDM process. It is a filament based process in which the filament itself is melted. Two different nozzles extrude and deposit material for creating part and support, where it is required. Diameter of the nozzle is typically 0.3 mm. Support material can be removed manually or can be dissolved in water based solution. FDM machines are sold by Stratasys [8], [9]. With this technology it is possible to produce not only polymeric materials parts, but also polymer matrix composites.

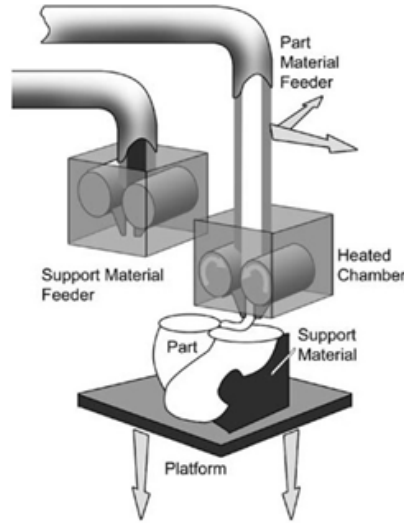


Figure 2.8: Fused Deposition Modeling (FDM) technology [7]

### 2.2.3 Examples of materials for AM/3D printing

In addition to the polymeric materials cited above (UV-curable resins, thermosets, etc.), many other materials were investigated for 3D printing, such as Polymer Matrix Composites (PMCs) and some kind of ceramics.

**Polymer matrix composites (PMCs)** In the most recent literature advances a wide range of applications of AM technologies is the production of polymer matrix composites (PMCs) which require a synthesis in liquid phase. Polymer powders and ceramics are mixed and laser sintered to form the composites, e.g., PCL and HA [9], PEEK and HA [10], PE and HA [11], PA and nanoclay [12], PA and SiC [13], etc. It has been found that polymethyl methacrylate (PMMA)-coated HA powder could facilitate better binding of the composite, but uncoated powder is used for the reason of biocompatibility. Coating of a powder has certain other advantages. In case of a nano-  $\text{Al}_2\text{O}_3$  and PS composite, nano- $\text{Al}_2\text{O}_3$  particles are coated with PS to prevent the agglomeration of nanoparticles resulting in a uniform distribution of particles in the polymer matrix [14]. The reinforcement powder is used in the form of particulates because fibers as a reinforcement give problems during formation of a smooth powder bed and are not helpful in increasing the final density and strength. Instead of taking a mixture of a polymer powder and a reinforcement powder, a single composite powder can also be used, e.g., glass-filled PA powder, Al-filled PA powder [15], [16]. HA - filled high density polyethylene (HDPE) powder, tricalcium phosphate (TCP) glass powder, etc. A single composite particle helps overcome the difficulty associated with mixing the powders and yields a uniform spread of composite components in the final product. However, if one of the components of the composite powder is a fiber, problems of manufacturing occur.

**Ceramics** Ceramic materials are conventionally synthesized through the solid state sintering route. However they could be also produced by AM in two different ways: (1) by directly processing a mixture of ceramics so that low melting point ceramic will melt and join others and (2) by processing polymer and ceramics so that the polymer will melt and bind the ceramics (these are referred to as liquid phase sintering). The example of the first type is Selective Laser Melting (SLM) - this technology mainly used for metals is widely discussed in chapter 3 - of PZT followed by furnace treatment [17]. In another example, a mixture of 70% TCP and 30% borosilicate glass was spray dried and used. During processing, the glass was melted and joined the phosphate [18]. In all these cases, porous products are formed.

There are many examples for the second type and is the most prevalent one to process ceramics at the moment. Notable example is phenol-coated sand where phenol coating is melted to bind remaining sand. It is used for making casting molds and cores [19]. Another one is the processing of a mixture of acrylic binder and glass powder. Acrylic binder melts and binds glass powders [20]. In all these cases, postprocessing by sintering in the furnace is done to either densify or crystallize the ceramics.

In the second type, polymer remains the part of the product but its amount is not high. In some cases, when the percentage of polymer is high or it is infiltrated during furnace treatment, the product is considered a composite.

## Chapter 3

# Additive Manufacturing for metals

### 3.1 AM technologies for metallic materials

AM systems for metallic materials processing can be usefully classified in terms of material feed stock and energy source which is used. A list of machines manufacturers which presents their equipments is reported in table 3.1 [21]. In this table, the presented systems are divided in three broad categories: powder bed, powder feed, and wire feed equipments. As can be seen the energy sources (electron beam, laser beam, plasma arc, etc.) for the different systems are described too.

System	Process	Build volume (mm)	Energy source
<u>Powder bed</u>			
ARCAM (A2)(a)	EBM	200 × 200 × 350	7 kW electron beam
EOS (M280)(b)	DMLS	250 × 250 × 325	200-400 W Yb-fiber laser
Concept laser cusing (M3)(b)	SLM	300 × 350 × 300	200 W fiber laser
MTT (SLM 250)(b)	SLM	250 × 250 × 300	100-400 W Yb-fiber laser
Phenix system group (PXL)(c)	SLM	250 × 250 × 300	500 W fiber laser
Renishaw (AM 250)(d)	SLM	245 × 245 × 360	200 or 400 W laser
Realizer (SLM 250)(b)	SLM	250 × 250 × 220	100, 200, or 400 W laser
Matsuura (Lumex Advanced 25)(e)	SLM	250 × 250 diameter	400 W Yb fiber laser; hybrid additive/subtractive system
<u>Powder feed</u>			
Optomec (LENS 850-R)(f)	LENS	900 × 1500 × 900	1 or 2 kW IPG fiber laser
POM DMD (66R)(f)	DMD	3,200° × 3°, 670° × 360°	1-5 kW fiber diode or disk laser
Accufusion laser consolidation(g)	LC	1,000 × 1,000 × 1,000	Nd:YAG laser
Irep laser (LF 6000)(c)	LD		Laser cladding
Trumpf(b)	LD	600 × 1,000 long	
Huffman (HC-205)(f)	LD		CO <sub>2</sub> laser cladding
<u>Wire feed</u>			
Sciaky (NG1) EBFFF(f)	EBDM	762 × 483 × 508	> 40 kW @ 60 kV welder
MER plasma transferred arc selected FFF(f)	PTAS FFF	610 × 610 × 5,182	Plasma transferred arc using two 350A DC power supplies
Honeywell ion fusion formation(f)	IFF		Plasma arc-based welding
Country of Manufacturer: (a) Sweden, (b) Germany, (c) France, (d) United Kingdom, (e) Japan, (f) United States, and (g) Canada			

Table 3.1: Main AM equipment providers with the corresponding specifications [21]

Figure 3.1 shows a schematic of a generic powder bed system, which could help to visualize how they work. A bed is created by raking the powders across the processing area. The energy source (electron or laser beam) delivers energy to the surface of the bed, melting or sintering the powder into the programmed shapes. The raster scanning of the surface is performed according to certain possible paths, the so called scanning strategies, which are generally provided by the manufacturers. The advantages of these systems include their ability to produce high resolution features, internal channels, and maintain dimensional control. Later on the most important technologies from this category are going to be discussed in detail: Electron Beam Melting (EBM), Selective Laser Sintering (SLS) and Selective Laser Melting (SLM), commercially known also with the trademarks, like Direct Metal Laser Sintering (DMLS) by EOS-GmbH company (Germany), or Laser CUSING, by Concept Laser GmbH.

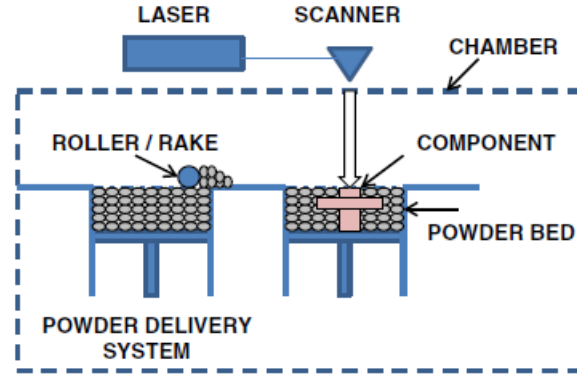


Figure 3.1: Representation of an AM powder bed equipment [21]

In addition to the powder bed systems, also powder feed equipments are commonly used. The scheme of a generic AM powder feed equipment is illustrated in figure 3.2. The available build volumes of these systems are generally larger than the powder bed ones. In this category of technologies, powders get conveyed through a nozzle onto the build surface. A laser is used to melt a monolayer or more of the powders into the desired final shape. The two main kind of available processes are:

1. the work part is stationary and the deposition head moves during the fabrication;
2. on the opposite, the head is stationary and the work piece moves.

The advantages of these last systems include the possibility to be used to repair worn or damaged components. Laser Engineered Net Shaping (LENS) process, which is powder feed based, is going to be discussed later on.

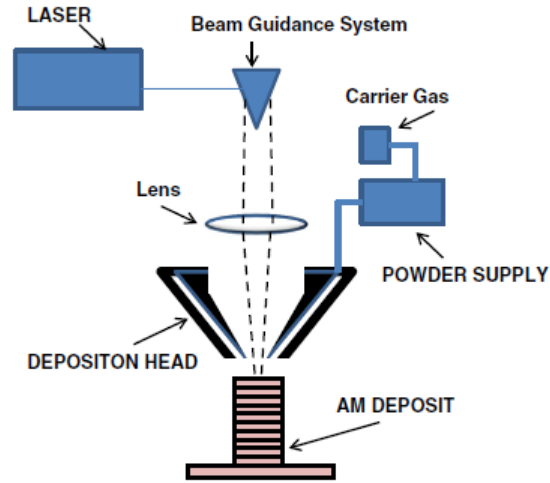


Figure 3.2: Schematic of an AM powder feed system [21]

### 3.1.1 Electron Beam Melting (EBM)

The localized melting of the material, deposited in a powder bed form, can be achieved by an electron beam instead of the focused laser. The procedure is then called electron beam melting, EBM. Since electron beam material processing requires a vacuum working area, a completely sealed type of machine is mandatory. Arcam AB (Sweden) presents a family of EBM machines dedicated to special applications, such as aerospace, medical, or tooling - the A2 system is shown in figure 3.4, on the left side. The electron beam penetrates very deep into the bed, then the process is very fast and it reaches elevated temperatures, also the building chamber is maintained at high temperature. As a result, stress and distortion are reduced and very good material properties can be achieved. Figure 3.3 illustrates an example of a structural component produced by EBM.



Figure 3.3: An example of a TiAl intermetallic turbine component by EBM [22]

The electron beam is emitted from a heated tungsten filament - see figure 3.4 on the right. The emitted electron beam is focused by a magnetic field. The focused electron beam is deflected to the required position on the build platform by another magnetic field. The electron beam interacts with the metal powder on the platform. The kinetic energy of the electron beam is so converted to heat and melts the region of the metal powder.

Higher energies get involved in EBM with respect to SLS/SLM technologies, because the electron beam is a more powerful energy source in comparison with the laser beam.



Figure 3.4: Electron beam melting, EBM: System A2 ARCAM (Sweden) on the left, and EBM process scheme, right [23]

The powder layer is preheated by an electron beam at high speed (2 m/s). Preheating of the powder layer is required to reduce the residual stresses that cause the warping of realized parts. After the preheating gets completed, the electron beam selectively melts at less speed (0.5 m/s) the powder bed according to the sliced file of the CAD geometry. A gas pressure of  $10^{-3}$  Pa is maintained in the electron gun and the process chamber is maintained at 1 Pa - you think that the normal atmospheric pressure is about  $10^5$  Pa. Moreover, a very low pressure of helium gas is then supplied in the process chamber to avoid the build



up of electrical charges in the processed metallic powders [24].

EBM process enhances the material properties due to processing in vacuum environment. EBM can process tool steel, Co-Cr alloy, Ti6Al4V alloys and Ni based super alloys. The parts produced in EBM process are used as propulsion exhaust system, high temperature bearings, biomedical implants and jet engine parts. However, the EBM process has some limitations such as process stability, part defects (in particular high surface roughness), quality variations and size of the building chamber [24].

### 3.1.2 Laser Engineered Net Shaping (LENS)

Among the powder feed based technologies, Laser Engineered Net Shaping (LENS) is an AM process in which the metal powder is fed in a gas jet through nozzles. This process is also known as Laser Cladding, Direct Metal Deposition (DMD), direct light fabrication or laser consolidation.

A schematic of LENS process is illustrated in figure 3.5.

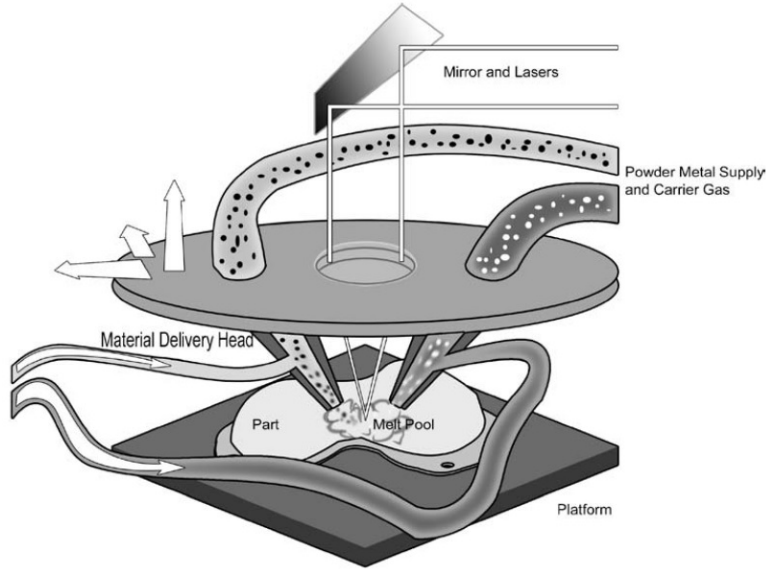


Figure 3.5: Schematic representation of the LENS process [6]

The platform is fitted to the table that moves in x/y plane. The z axis movement is provided to the laser as well as to the powder nozzle unit. Figure 3.6 reports an example of the deposition of 316 stainless steel powder in single-line build [29]. The powder is normally delivered coaxially with the laser beam, or in other words perpendicular to the build platform. The powder material is melted due to the interaction of laser beam. The molten material is deposited

on the platform, based on the sliced geometry of the original CAD data as usual. The process occurs in inert gas atmosphere - less than 0.001% of  $O_2$  concentration is required. After the part building is built up by this technology, the part can be heat treated, hot isostatic pressed or machined to suit the requirements of the specific application. LENS process is used for AM of parts, repairing work such as fixing mould tools and also for coating purposes [6], [7], [25], [26], [27]. This process has been commercialized by POM, Optomec, Aeromet and MTS companies. Titanium alloys, nickel based superalloys, steels, cobalt-chromium alloys and aluminium alloys can be processed in LENS [7], [28]. LENS process offers a very fine microstructure while consolidating the metal powder. This results in higher tensile strength and ductility of metallic parts than conventionally produced ones [8], [28].

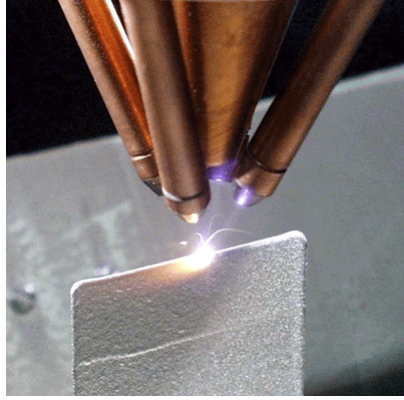


Figure 3.6: Example of LENS application [28]

LENS process provides the following advantages:

- it can produce fully dense metal parts with good metallurgical properties at reasonable speeds;
- novel shapes, hollow structures, and material gradients that are not otherwise feasible, could be reasonably built by LENS;
- this process is also able to add features to cast or forged parts [7], [28].

However, the main limitation of LENS is the complexity of parts that could be realized. The overhang angle which can be built is usually greater than  $30^\circ$  from the vertical. There are few more problems with this process, namely the microstructure control, dimensional accuracy, controlling thickness of the material deposited, high surface roughness of the final parts ( $40 - 50 \mu m$ ) of the parts and residual stresses present in the parts [7], [28].

### 3.1.3 Selective laser sintering (SLS)

Among the powder bed processes, the selective consolidation of thermoplastic powders is called laser sintering or selective laser sintering. Sintering processes in general do require neither bases to build the parts on, nor supports to link the parts to the bases, because the loose powders surround and stabilize the parts during the building. Concerning polymeric materials this is true, whereas metal parts represent an exception. In fact, support structures are required, mainly to prevent the parts from warping during the build process. Moreover, in the processes for metals, supports are fundamental to bring away the heat in excess due to the strongly localized energy source.

Nowadays, the term laser sintering or selective laser sintering (SLS) is used preferably for machines that process thermoplastic materials. They consist of a build chamber to be filled with powder with a grain size of up to  $50\text{ }\mu\text{m}$  and a laser scanner unit on top. The bottom of the build chamber is the build platform, which is mounted on a movable piston and so it can be adjusted at any z coordinate - as it is shown in figure 3.7. The top of the powder bed defines the build area in which the actual layer is built, and the process chamber gets completely flooded by a shielding gas in order to prevent oxidation.

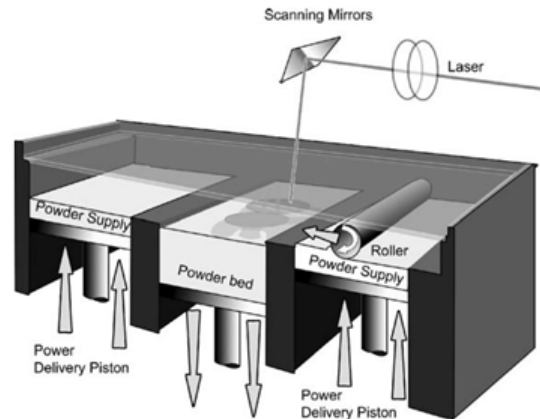


Figure 3.7: SLS scheme: melting and solidification of a single layer, lowering of the platform, and successive recoating [6]

The SLS process follows these main steps in a loop:

1. A substrate, so the build platform, is lowered down to a depth equal to a single layer thickness;
2. a powder layer is deposited on the substrate;
3. the spread powder layer is raster scanned by the laser beam to melt the powders together when and where it is required.

This sequence is repeated until that the fabrication of products is complete. In the initial stage of the process, powder is placed in a powder container and it is compacted there. Adjacent to the dispenser container is placed a scraper, which carries the powder toward a substrate (the so called build platform). The containers are placed on pistons so that their vertical position could be changed. A scanning mirror is used to focus the laser beam coming from the laser source on the deposited layer.

According to the scheme reported in figure 3.8, in step 1 of the sequence, the motor of the powder container moves upward of a layer thickness and the piston of the substrate container moves equally downward. This step gives requisite powder to be carried away by scraper, or recoater, and volume on the build platform for the powder to be deposited. In step 2 of the sequence, powder is deposited over the substrate and the position of the scraper changes towards the right of the build platform. In the last step (step 3), deposited powders are scanned by laser beam. After each deposition step, the excess powder carried away falls into trash (the so called collector platform) equipped at the right side of the build chamber in this representation.

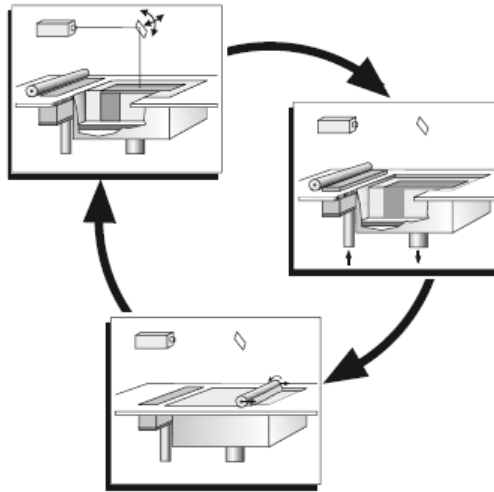


Figure 3.8: A schematic representation of SLM process [29]

The above description shows the basic necessities of the process:

1. formation of the powder bed;
2. consolidation of powders by laser beam;

3. a mechanism that allows to repeat the steps.

The description above applies also to Selective Laser melting (SLM). The term SLS is used for polymers even in case of full melting: it is mainly because a certain level of residual porosity is always present. On the contrary, SLM is properly used with reference to almost fully dense obtained parts. SLM was investigated in subsequent paragraph 3.2, in terms of involved mechanisms, microstructural characteristics of the processed materials, by reviewing the available scientific literature.

## 3.2 Selective Laser Melting (SLM)

SLM strictly refers to the cases in which full melting of powders occurs, obtaining dense parts. SLM traces its origin back in 1986 when a master student of University of Texas filed a patent on it, which got granted in 1989. The process was later commercialized by DTM corporation which is now part of 3D Systems, and since then the process has seen an exponential growth in all aspects: related patents, types of materials processed, scientific papers published and presented, new possible applications, machines sold, new companies and institutions that adopted it for research and production.

The process generally occurs in a nonoxidative environment maintained by the presence of nitrogen or argon gases and the temperature of the build platform is increased from room temperature. In fact, controlling the atmosphere in a process chamber has two aims: (1) to make it free from any contamination and (2) to prevent oxidation. Nitrogen gas is used for most engineering materials to prevent oxidation reaction, but in case of titanium and aluminium, argon gas is mandatory. Oxidized layers or powders have a reduced tendency for wetting with the fresh molten metal: this is going to result in an increased final porosity and so decreased density. Nitrogen gas is not used for titanium because it forms titanium nitrides at high temperature. Hydrogen gas is also not preferred because it can lead to hydrogen embrittlement [29].

Flowing the gas parallel to the optics plane is also used to protect the optical apparatus from particles condensing on it [30]. The powder feeding amount, deposition system, raster scanning, temperature, atmosphere and build process are computer controlled.

### 3.2.1 Mechanisms involved

In order to understand and identify the main parameters which play a key role in the SLM process, it is fundamental to explain the mechanisms involved.

Initially, all contour of the layer structure of a part gets exposed with a selected laser power and contour speed. As the diameter of the melted zone is usually larger than the laser diameter, it is necessary to compensate the dimensional error and the laser beam must be shifted by half width from the contour to the inside, to make sure that the contour of the later part will correspond exactly to the original CAD data [3]. This correction of the position is called

beam offset [31]. The beam offset value is again defined with respect to the edge of the boundary, and if this value is higher or less than the correct value, the particles of the irradiated region may be not melted or supermelted - you can refer to the scheme reported in figure 3.9. During hatching, the laser beam so moves on line after line. The distance between the lines is called hatching distance ( $h_d$ ) and is generally set about one quarter of the laser beam. Another important parameter that can lead to a distorted part or a process interruption is the layer thickness ( $d$ ). If the value is too high, no optimal adhesion between the single layers can be obtained since the melting depth is not high enough. Furthermore, mechanical stresses can generate through this layer which can lead to detachment of the layer below. On the opposite, if the selected value is too small, a tearing-off of a structure can happen during the recoating process, since the melted particles get struck between it and recoater blade [32].

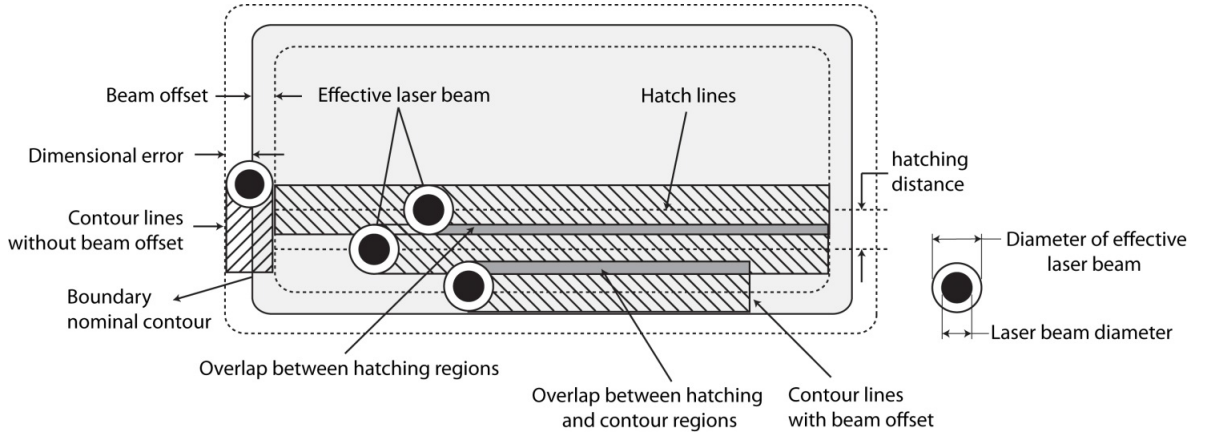


Figure 3.9: Schematic of the hatching mechanism by the laser beam [3], in particular in DMLS process of EOS

Many scanning options are provided in commercial SLM machines. Moreover, depending on the manufacturer the possible scanning strategies would change. In fact, significant differences in the scanning strategies can be observed between Laser CUSING by Concept Laser GmbH and DMLS by EOS GmbH. Laser CUSING has the stochastic exposure strategy in line with the “island” principle [33], whereas DMLS has the skywriting and the hatch pattern along  $x$ ,  $y$ , both in  $xy$  and alternating in  $xy$  for different requirements.

DMLS machines by EOS GmbH present up-skin and down-skin options to improve mechanical properties by allowing the adopter to assign different process parameters at adjoining layers. In chapter 4, which is entirely dedicated to the EOS GmbH equipment and technology in use in this PhD thesis work, the graphs are going to illustrate salient features of scanning strategies available with DMLS process.

Although the direct laser sintering/melting technology can be applied to

a broad range of powders, the scientific and technical aspects of the production route such as sintering rate and the effects of processing parameters on the microstructural evolution during the layer manufacturing process have to be well understood. SLM is accompanied by multiple modes of heat transfer, and chemical reactions which make the process very complex: in 2003 Fischer et al. wrote that the method essentially relied on empirical and experimental knowledge [32]. The potential benefit from improved knowledge was related to advances of intelligent process control and automation as well as to allow operators to select proper parameters value before processing [34]. More recently, many literature works have been performed to develop models for SLM process.

Concerning the understanding of the occurring phenomena, it is relevant to discuss which kind of binding mechanisms regulate the process. More in general, these are the possibilities according to Kruth et al. [4]:

1. solid state sintering;
2. liquid phase sintering or partial melting;
3. full melting, specifically occurring in SLM.

Solid state sintering occurs, when the particles are heated to a range between  $T_{\text{melt}}/2$  and  $T_{\text{melt}}$ , where  $T_{\text{melt}}$  refers to the melting temperature. This mechanism is suitable to describe the conventional sintering process for ceramics. Reducing the total free energy of the particles is the driving force solid state sintering. The mechanism of sintering is mainly the diffusion between the powder particles. Neck formation between the adjacent particles occurs due to the solid state sintering - you can refer to figure 3.10.

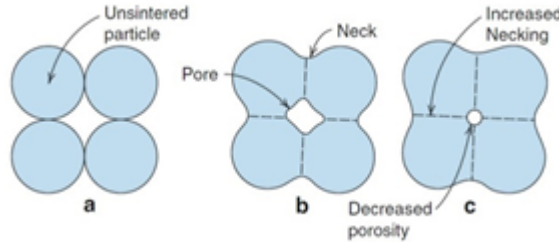


Figure 3.10: Conventional sintering among ceramic particles [4]

Liquid phase sintering provides higher dimensional accuracy to the built parts. Consolidation through this mechanism happens in two ways: (1) making a porous product followed by densification and (2) making a final green product. An example of the second type is DirectSteel powder supplied by EOS GmbH. This is an iron based system, which contains iron and copper phosphides. During processing, phosphides melt and join remaining components of the powder. It

provides about 95% density and sufficient mechanical properties to be used as a mold [35]. It is clear that it is not possible to obtain pore-free products using this kind of mechanism.

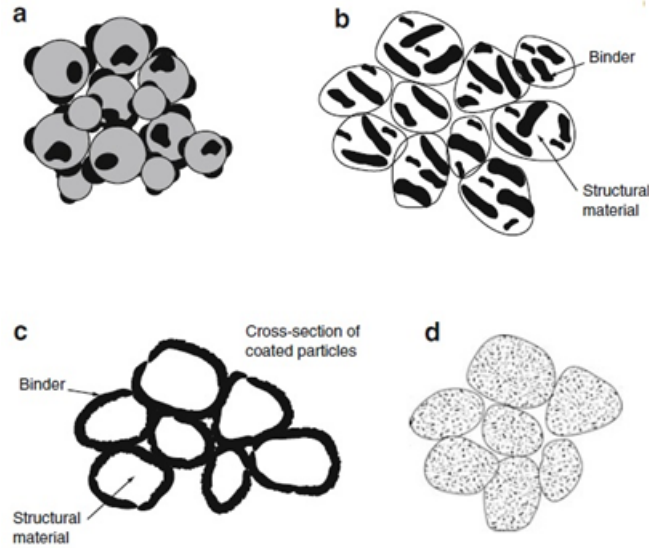


Figure 3.11: Liquid phase sintering [4]

Figure 3.11 (b) depicts the composite particles case. Composite particles can be obtained by mechanical alloying of two different powders. The binder material is coated on the structural phase in coated particles, as shown in figure 3.11 (c). The use of coated particles assures the laser energy is absorbed by the binder material. The binder phase can be of polymer or metal. For instance Cu coated steel particles, polymer coated metal particles could be feasible solutions [35], [36]. Polymer coated metal particles require debonding of polymer after laser sintering, then post infiltration is carried out (again SLS).

Full melting is finally the main binding mechanism governing SLM. To achieve completely dense metallic parts SLM machines that use diode pumped Nd:YAG, fiber or disc lasers have been developed. The heat energy of the laser beam melts the whole region of the powder material to a depth exceeding the single layer thickness.

Due to this, previously solidified structure is also re-melted, and this entails the formation of specific affected volumes, which are detectable as the identifying microstructural marks of a metallic material by SLM in general: you can observe the result of the formation of molten volumes in correspondence to the laser beam wipes along the building direction, the so called “scan tracks”, and these are known in the literature as melt pools.

The main driving force for using full melting is to realize pore-free products, fast production, and high strengths.



There are a number of researches on iron-based, titanium-based, and nickel-based alloys. In addition many other alloys and metallic systems such as cobalt-based, aluminum-based, magnesium-based alloys, copper, silver, and gold are getting investigated. Due to high laser scan speed, the process gives high cooling rate (about  $10^6$  °C/s) [4], which helps to form very fine microstructures.

Therefore, the full melting mechanism is very effective to synthesize high density structures from engineering metals [35]. However, the full melting also has drawbacks which need to be faced:

- high internal stresses or warping of a part is induced due to the high temperature gradients and densification ratio (50% powder porosity to almost 100% density in a single step);
- the risk of balling and formation of dross in the melt pool may cause poor surface finish [60].

### 3.2.2 Microstructural properties after SLM

The microstructure and phases formed can be controlled by process parameters, in particular such as laser power and scan speed, which provide desired mechanical properties, strength and ductility. It has been found that properties are better than conventionally produced components: in fact higher strength combined with higher ductility is found in SLM products [36]. Changing the build direction of a part causes a change in the amount and direction of columnar grains responsible for changed properties [37], [38].

Figure 3.12 illustrates a schematic representation of the melt pools and shows the characteristics which help to define the scan tracks. Gusarov and Smurov (2010) proposed a way of calculation of the melt pool shape and dimension by an accurate model calculation: the effective radiative properties of powder beds depend on the morphology and the size distribution of particles through their specific surface. The stability of the SLM process depends so on the scanning velocity, powder layer thickness, and the material optical and thermal properties [40].

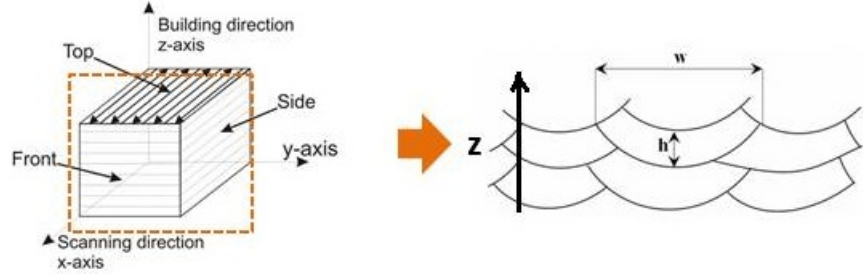


Figure 3.12: Micrograph of specimen with scan tracks oriented in the x/y plane, and nomenclature of scan tracks, where  $w$  = width of scan track and  $h$  = height of scan track [5], [39]

As explained by Yadroitsev et al. [41], the formation of single scan tracks from metallic powder by SLM has a threshold character: for each powder material in use, there exist sets of process parameters which yield stable or unstable tracks. The mechanism of distortion, defects and drops formation might be associated with thermophysical properties of the material, granulomorphometric properties of the powder, peculiarities of its deposition and the spreading during the repeated recoating phase (the concept known as flowability), layer thickness, energy parameters of laser beam, raster scanning speed and melt hydrodynamics.

In addition, different scanning strategies lead to different final outputs: the choice of the proper scanning strategy is then fundamental (you can read more in chapter 4 concerning the different building strategies). As stated before, SLM microstructure is a result of extremely fast solidification and its features correlate with heat conducting direction.

For example, it is very important to compare the microstructure and mechanical properties of SLM parts from Ti6Al4V, the most commonly used titanium alloy for high performance engineering solutions, with the appropriate quality standards of this material and its products from wrought or cast alloy for biomedical applications [42]. In figure 3.13 you can observe the presence of fully martensitic fine grains in the microstructure of Ti64 alloy by SLM in comparison with the microstructure of the same alloy obtained by a conventional technology such as forging: in the conventionally processed material  $\alpha$  phase is lighter and the  $\beta$  phase is darker. The shown as built SLM sample from Ti6Al4V by SLM presents a very fine martensitic microstructure with a texture in the built direction. Yadroitsev et al. monitored the local radiation area phenomena, in particular the correlation between the presence/absence of certain phases and the reached temperatures during SLM [43]. Figure 3.14 shows the microstructure of a post heat treated sample from Ti64: the heat treatment was performed to achieve a higher ductility and to reduce the thermal stresses

generated during the process [42].

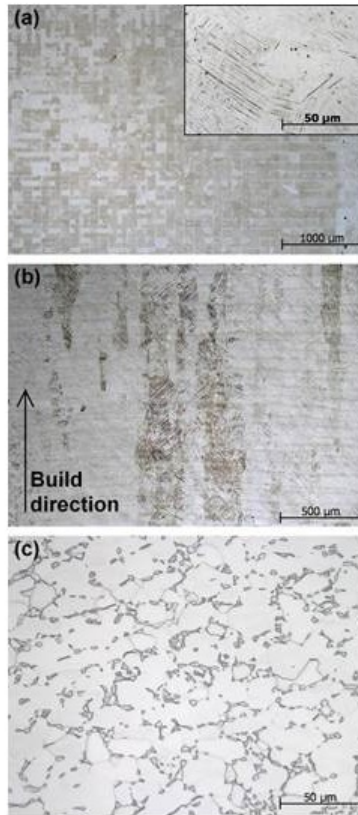


Figure 3.13: Top (a) and side (b) view of as built Ti6Al4V realized by SLM. In (c) the optical micrographs of the reference material obtained by forging [43]

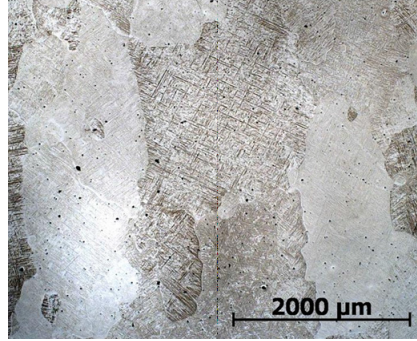


Figure 3.14: After heat treatment at 1015 °C for 2 h, water quenched, indicating the extensive growth of the columnar grains [41]

Fischer et al. published a very complete work on commercially pure titanium, which combined the numerical simulation of heat flow during the process and the experimental data acquired from sintering titanium plates [32].

On the other hand, concerning nickel based superalloys, for instance Inconel 718 [44] and 939, they have been intensively used in high temperature service applications (energy and aerospace sectors). However, the conventional techniques are limiting their use, among which excellent oxidation resistance and high creep strength at elevated temperatures. For this reason SLM could be particularly suitable. In figure (a) arch - shaped lines resulting from an equally shaped melt pool during processing are clearly visible (the analysed sample is from Inconel 939). In figure (b) in the plane perpendicular to the building direction, the scan tracks appear elongated which is correlated to the laser beam scanning paths [45].

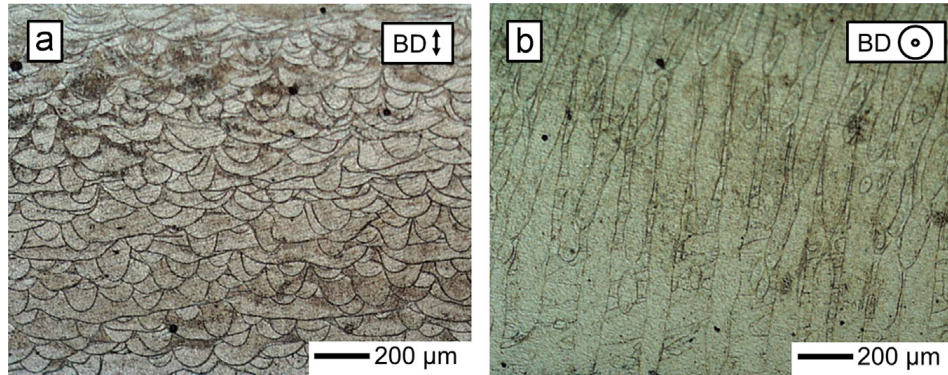


Figure 3.15: Optical micrographs from Inconel 939 by SLM: the images were recorded parallel (a) and perpendicular (b) to the building direction

Moreover, the mechanical properties of Inconel 939 were characterized [45]:

the yield strength results higher than that of the cast material, due to the refinement of the grains. A similar work was published concerning another nickel based superalloy by Song et al. using an “open” commercial SLM system, to realize parts for mechanical and structural characterization from Ni20Cr powder [46].

Monroy et al. instead used a self - developed SLM machine to realize samples from CoCrMo alloy, by considering a Design of Experiments (DOE) taking into account the usual process parameters, with the aim to study the porosity/density level in the material processing. The optimal process window to reduce total porosity level at about 1% was found out [47].

In addition, another investigated material was Nitinol : it is known to be a peculiar NiTi intermetallic phase characterized by some interesting properties: biocompatibility, superelastic behaviour and a shape memory effect. Shishkovsky et al. studied the feasibility of fabrication of 3D dense parts made from nitinol via SLM [48]. Figure 3.16 shows optical micrographs of a NiTi polished sample fabricated by SLM. The laser passage strips in the vertical direction in 3.16 (a) can be observed. The Nitinol remelted microstructure from the lateral side - figure 3.16 (b) - presents elements characteristic of the multi-pass laser, as well as few residual pores or small cracks.

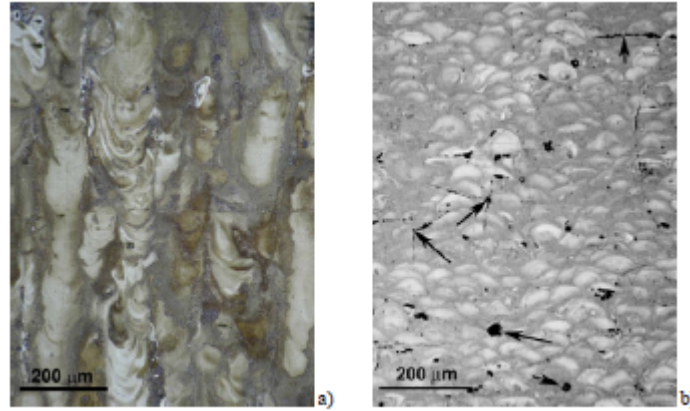


Figure 3.16: NiTi frontal (a) and lateral (b) optical micrographs [48]

On the contrary iron based materials were extensively studied in the past and many traditional processing methods could already provide iron parts. However the research and exploration about processing methods of iron based alloys has been continuing, to realize different very complex shaped iron molds and some kind of unconventional designs. Simchi et al. studied the effects of SLM processing parameters and the role of particles on the microstructure and densification of iron powders [49-50]. Murali et al. reported the role of graphite addition in

SLM technology of iron powders [51], and Kruth et al. contributed by studying the influence of SLM parameters on density of iron parts [52]. Nearly dense parts can be obtained by properly adjusting parameters and then applying the optimized process window. Thanks to the decrease of the average grain size (refinement) the tensile strength of SLM fabricated iron specimens was much higher than that of the conventional iron [53]. Yan et al. investigated the performance of advanced stainless steel 316L cellular lattice structures realized via SLM and then characterized by elastic field compression testing [54]. Similar work, in particular in terms of characterization of the microstructure at a very little scale, with respect to titanium based systems, was performed by Liu et al. in the analysis of M2 high speed steel (HSS) [55]. Ferritic, austenitic and martensitic phases were observed to be present in the M2 HSS samples. Three different zones, A, B and C identified from the Focused Ion Beam (FIB) imaging - taken along the melt pool boundary to indicate the different phases present - are shown in figure 3.17. Zone A is characterized by ferrite phase, whereas zone B is characterised by a mixture of disoriented austenitic and ferritic phases, and lastly zone C, on the other hand, is characterised by a disoriented mixture of ferritic, austenitic and martensitic phases. Zone C displayed acicular martensite features that are characteristic of tempered M2 steel. Since the SLM process is a layer by layer additive manufacturing process, the material in each layer was influenced by the laser during the SLM process and experienced a thermal condition where partial tempering took place resulting in formation of martensites.

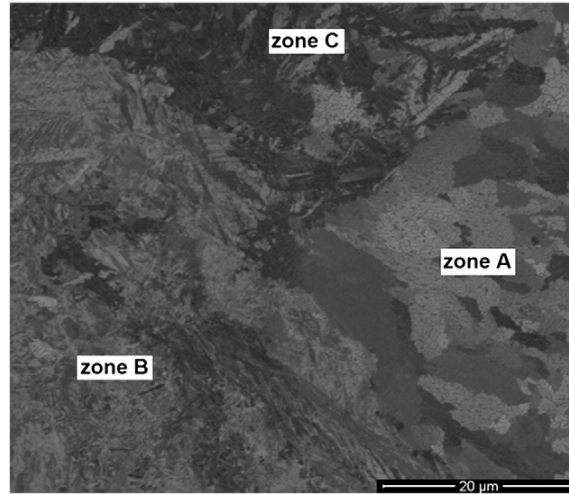


Figure 3.17: Optical images from an M2 HSS sample by SLM [55]

Concerning then aluminum alloys by SLM, first investigations gave evidence that it is possible to achieve a high level of density with AlMg3, AlMgSi0.5, AlSi12 and AlSi10Mg alloys [56]. Even though many manufacturing companies provide aluminum powders systems, the range of aluminium alloys suitable to

be processed via SLM is relatively small: mainly AlSi10Mg and AlSi12, since the most important aspect to be considered is the castability of the aluminum alloy itself. In order to build dense parts, it is fundamental that the melt pool does not consist of different subareas but is cohesive and self contained. Buchbinder et al. proposed to setup a machine with a 1 kW maximum laser power with a multi beam system [39]: in figure 3.18 a micrograph of AlSi10Mg along the build direction is illustrated.

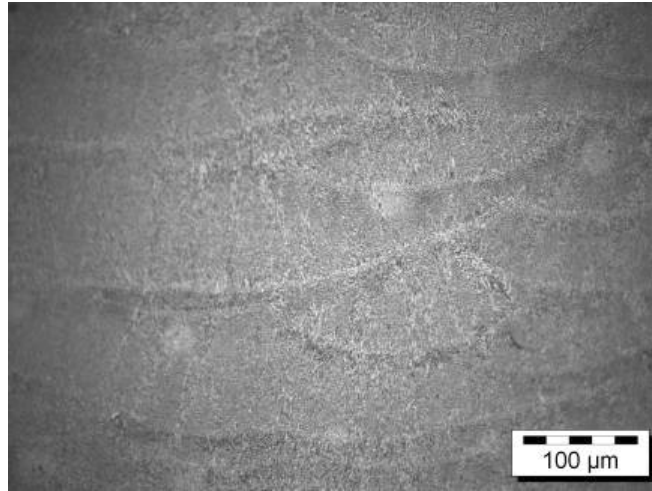


Figure 3.18: Optical micrograph of AlSi10Mg sample by SLM [39]

Brandl et al. [57] affirmed the crucial role of process parameters on the microstructure, cycle fatigue, and fracture behaviour of AlSi10Mg processed powders, by showing that the combination of 300 °C platform heating and peak - hardening increased the fatigue resistance and homogenise the microstructure. Furthermore, Olakamni et al. [58] employed the concepts of laser absorptivity, heat conductivity, fluidity of the molten volume and the powder's oxide content to explain the oxide disruption phenomena in SLM of pre - alloyed Al - Mg and Al - Si powders when process parameters were varied. Olakamni et al. [59] also explored the role of the processing parameters on the densification mechanism and microstructural evolution in laser sintered Al - Si12 concluding that the laser energy input is the determining factor. They also suggested that the tops of the grains in the previous layers get partially remelted and then undergo epitaxial growth in the next layer where the heat affected zones (HAZ) grain boundaries and solidification grain boundaries are continuous along the fusion boundary. Thijs et al. [60] characterized pre-alloyed AlSi10Mg and the experimental results showed that the high thermal gradients occurring during SLM lead to a very fine microstructure with submicron-sized grains.

In the context of the aluminum alloys, the efforts from the research group in which this PhD activity was pursued, brought to different publications [3,5,31,69,97,98].

In particular, this thesis aims:

- to characterize AlSi10Mg alloy by DMLS realized with an EOSINT M270 Xtended version machine by EOS GmbH, which is “open access”, so allows the proper optimization of the process parameters for each different material. The characterization was mechanical and microstructural;
- to develop, investigate and characterize two different Aluminum Matrix Composites (AMCs) based on the alloy previously studied. The first one was obtained by mechanically alloying 10% in weight of submicrometric SiC to the matrix, whereas the second was by addition of 0.5% in weight of nanometric  $\text{MgAl}_2\text{O}_4$ .

### 3.2.3 Main SLM parameters

It is fundamental to discuss the laser radiation coupling into material, in particular the interaction with granulated material.

The physical processes associated to laser melting include heat transfer and joining the powders together. Recently, many works have been performed to develop computer models for the laser sintering process [61-64]. Although modeling of laser sintering rates for real systems is difficult and in many cases may not provide accurate results, isothermal sintering rates of amorphous materials can be used. For instance, Nelson et al. [65] assumed that the sintering rate is a function of temperature according to Arrhenius equation. Sun et al. related the sintering height to the laser power and laser velocity by simple empirical equations [66]. Cervera et al. considered the powder bed as an open pore network of cylinders and evaluated the sintered density as a function of time and temperature according to the Mackenzie - Shuttleworth model [67]. Unlike polymer materials, liquid phase sintering and melting/solidification approach are the mechanisms feasible for rapid bonding of powder particles in the SLM [68]. As it was cited at the beginning of chapter 3, SLM is also known with its trademark by EOS GmbH company.

The size distribution of the powders determines the minimum layer thickness, which is either smaller than or equal to the desired layer thickness. For instance, we could not deposit a layer of 20  $\mu\text{m}$  thickness using powder of about 100  $\mu\text{m}$  mean diameter.

In addition, concerning flowability of the powders, they should have the following properties in order to be successfully processed by SLM: spherical in shape, low surface roughness, narrow powder size distribution, incompressibility, high density, hard and stiff so that it would not be deformed and shape change would not occur.

If the material, in particular aluminium and copper, presents high reflectivity, it will reflect laser beam and it would be difficult to process the powder. However, powder bed has low reflectivity than a solid block because pores on the powder bed absorb the laser beam. Even then, for processing, reflective



material needs high laser energy. Absorption of the powder bed could be increased by adding material of high absorptivity, which will make the process energy efficient.

Laser power is one of the main parameters in SLM process. Its magnitude depends upon the type of materials processed. Nowadays the machines are equipped with laser sources of power ranging from 50 up to 400 W. The selection of power is not done independently, but depends upon other process parameters and the laser spot size. For the same laser power, with a decrease in spot size, higher laser energy density is achieved, which could be used to process higher melting point materials. Laser power also depends upon your aim with powders. If you want to completely melt it, then more power is required. If the aim is to melt the powder partially then less power is required, and this represents the case of SLS technology. Using higher laser power than required may evaporate the metallic powder. As a consequence, it is fundamental to find a “process window” for each material [69]. In order to carry out process control in the system, laser power has been mostly used as a controlling parameter to cause changes into the system: its optimization could then give rise to consistency in mechanical properties and dimensions of the realized parts [70-71].

CO<sub>2</sub> and Nd:YAG, among the solid state lasers, are the mostly used in SLS/SLM. The selection of the laser source depends on their power, mode of operation (continuous or pulsed) and their absorptivity by powder bed. Metals and ceramics (in particular carbides) absorb Nd:YAG more. In other words, smaller wavelength is absorbed by metals and their alloys [72-74]. Consequently, the machines made for processing polymers use CO<sub>2</sub>, whereas for processing metals Nd:YAG or Ytterbium fiber laser is used. In case of a mixture of powders, the selection of laser is governed by the type of powder primarily processed. For instance, in case of processing WC - Co mixture, where laser is used to melt Co to bind WC particles, Nd:YAG or fiber laser are suitable. It implies that in a given SLS/SLM system, the maximum scan spacing obtained is limited. In order to avoid any porosity formation at the boundaries of scans. Overlap is necessary because in a typical Gaussian beam, laser power at the center of the scan is higher than at the boundary of the scan resulting in melting at the center while heating at the boundary. Creating the overlap compensates this less heat generation at the boundary.

Scan speed in SLM determines the melt pool length. Higher scan speed gives rise to longer and thinner melt pool, which has more chance to break into several smaller melt pools (ball) due to Rayleigh instability [75].

Another important parameter directly related to the process is the already cited layer thickness. Through its increase, higher productivity is achieved, whereas with its decrease you have higher precision. Higher laser energy is required for processing thicker layer. However, there is a limit to which laser energy could be increased because supply of high energy sometimes causes distortion on the surface and gives rise to inaccuracy. This could be avoided by

scanning the same surface twice with lower energy.

These considerations brought Kruth et al. [4] to propose the following relation:

$$VED = \frac{P}{h_d s_s d}$$

where VED is the volumetric energy density, measured in J/mm<sup>3</sup>,  $s_s$  is the raster scanning speed of the laser beam,  $h_d$  is the scan spacing, and  $d$  is the layer thickness. This equation works when laser spot size is always larger than hatching distance. Lower layer thickness also means lower shrinkage after melting by moving laser beam, which will increase the dimensional accuracy and surface smoothness.

### 3.2.4 Systems and manufacturers

The successful implementation of the SLM process depends upon the commercial availability of a system, and its consequent level of spread. The importance of the process has been recognized since its inception leading to a number of manufacturers getting involved in developing the systems: research groups are getting more and more involved in the development of home made systems. Notable manufacturers are EOS GmbH (Germany), 3D Systems (USA), Concept Laser GmbH (Germany) and Phenix (France). Ghany et al. reported the comparison of four different SLM manufacturers taking into account a complete set of aspects [76]. Figure 3.19 shows a photograph of a system released by EOS GmbH whereas Figure 3.19 gives a closer view of its processing chamber. A system typically contains a powder container, powder deposition system, build platform, laser source, heating elements, inert gas supply, atmosphere sensors, and on board computer.

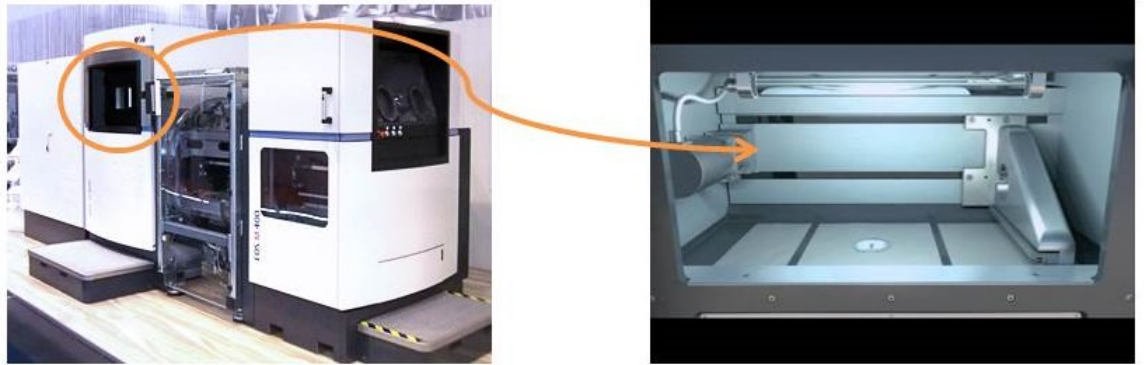


Figure 3.19: A sample of EOS GmbH system EOSINT M400 and a closer view of the process chamber [77]

They are explained briefly as follows: (1) Powder container is meant for keeping enough powder in the machine so that the built does not need to be interrupted for refilling the powder. (2) Powder deposition system is meant for depositing thin layers of powder on the build platform; this consists of roller/blade and piston. (3) Build platform is generally a parallelepiped bulk tightly fitted in its proper housing, it moves along z-axis in the housing using a motor, the movement distance is set equal to layer thickness, and build platform combined with parallelepiped housing is called build chamber. (4) Laser source is required for generating laser beam. (5) Scanning system is meant for scanning the powder bed, and the optics is selected on the basis of laser power, laser type, and the required maximum scanning speed. (6) Heater is meant to heat the powder bed and powder to a certain temperature; both induction and radiation types are used; they are used underneath the build platform or on the wall of the process chamber. (7) Vacuum pump is used to create vacuum in the process chamber. (8) Inert gas supply is required to maintain constant flow of inert gas in the chamber during the built. (9) Temperature sensor is used to note the temperature of the powder bed while oxygen gas sensor is used to note the amount of oxygen in the chamber. (10) Computer is used to set and control the various process parameters, it is equipped with necessary software to edit standard Tessellation language (.STL) files and monitor the properties of the layer during building process.

Recent versions of these type of machines are having higher build volume. The utility of this higher volume could be found in both the production of higher number of complex parts in the same run (the so called “job”) and of integrated structure philosophy, which replaces the need of joining and assembly of components. Bigger volume machine needs the same amount of powder even if a tiny part instead of a big part is fabricated. This gives rise to a large amount of powder to be recycled (up to 95% gets saved). Anyway, either for a small or big part, the time for powder recoating, atmosphere control, and preheating remains unchanged. This warrants the optimum utilization of the build volume.

New concept machines have been developed for few years, which contain smaller but more flexible build volumes: in fact, the build chamber contains pull-out drawer systems. Smaller missions are then suitable to fabricate for instance jewelry objects or small but very precise and unique parts: you could think of the dental implants, as reported by Gebhardt et al. [78].

### 3.2.5 SLM for Metal Matrix Metal Composites (MMCs) production

Recently, also processing of composite materials has attracted the interest due to the potential of the process in freeform fabrication of intricate articles in a reduced production cycle.

In general, the main reason for processing metallic based composites is to combine various materials for achieving specific properties unachievable by a

single material. The ex-situ approach is the most common method used for consolidating a metal matrix composite, since the basic principle is very simple: powdered metal and discontinuous reinforcement are mixed together and then bonded, through a certain process of compaction. On the contrary, in the so called in-situ approach, induced chemical reactions, for example by the laser radiation in case of SLM, are used to create in-situ the reinforcing phase during the realization of the composite itself.

**Ex - situ approach** This approach has widely been used to produce MMCs by SLM starting from different kind of matrixes. For example, Fe and graphite [79], WC-Co [80-81], WC-Co and Cu [82], Fe, Ni and TiC [83]. Addition of  $\text{La}_2\text{O}_3$  to the mixture of WC-Co and Cu decreases the surface tension of the molten blend and consequently increases its processability [83]. Moreover, strengthening of a WC and Co green product may be done by infiltrating it with bronze [80-81]. In table 3.20 a list of developed materials from the literature is reported.

Materials used
Fe, graphite
Ti, graphite/diamond
Ti, SiC
AlSi, SiC
AlMg, SiC
Co, WC

Figure 3.20: Materials used for the direct fabrication of MMCs by SLM [82]

Because of the complex nature of DMLS technology, some process defects associated such as balling phenomena and curling deformation are still difficult to completely overcome, and these negatively affect the produced parts.

Concerning aluminum matrix composites (AMCs), in general the ceramic materials most used as particulate reinforcements in the field of composites are  $\text{Al}_2\text{O}_3$ , SiC,  $\text{B}_4\text{C}$  and more recently also  $\text{TiB}_2$ , TiC emerged as potential candidates. Topcu et al. recently investigated the mechanical performances at high temperature of composites with different compositions reinforced varying weight percentages of micro- $\text{B}_4\text{C}$  particles, fabricated by powder metallurgy and subsequent sintering [84]. In 2008, Kerti et al. proposed a solution to promote the wettability between the ceramic reinforcement and aluminum melt during conventional casting [85]. In the case of DMLS process, silicon carbide was the most studied second phase, due to its interesting hardness, stiffness and thermal properties. In 2008 Simchi et al. published an investigation of AlSi7Mg0.3-SiC composites by DMLS [86]. Ghosh et al. in 2011 pursued a work based on mixing AlCu4.5Mg3 with SiC, but the results were not promising in terms of about 15% level of porosity in the final parts [87]. Moreover, in the Al-SiC system,

one of the most serious detrimental issues is the possible reaction between the aluminum matrix and the silicon carbide reinforcement.

**In - situ approach** The energy of the laser beam can be used in two ways: (1) to overcome the activation energy of the reactants and to form chemical compounds and (2) to trigger a chemical reaction that will not only form a compound but generate enough thermal energy to propagate chemical reactions. Both types of in - situ formation of compounds are better than the preaddition of compounds because of the following reasons: fine and uniform distribution of compounds, better wetting, and release of exothermic energy helpful to the binding. Examples of the first type are the formation of Cu - based MMC reinforced with  $\text{TiB}_2$  and  $\text{TiC}$  from a powder mixture of Cu, Ti, and  $\text{B}_4\text{C}$  [88] or Cu-TiC composite from Cu-Ti-C [89]. The second type is a case of self-propagating high-temperature synthesis, i.e. formation of  $\text{TiC-Al}_2\text{O}_3$  composite from  $\text{TiO}_2$ , Al, and C [90];  $\text{Al}_2\text{O}_3$ - Cu composite from CuO and Al [91]; and NiTi-HA composite from Ni, Ti, and HA [92]. In the latter case, it has been found that although the product is porous, it could be suitable as an implant material. Chemical reactions may also help creating a binder material in the case of laser processing of SiC, where disintegration of SiC and subsequent reaction with  $\text{O}_2$  gas forms  $\text{SiO}_2$ , which binds rest of SiC powders. This manufacturing mechanism has not furnished strong parts and has not been further used.

## Chapter 4

# Methods and characterizations

### 4.1 DMLS

#### 4.1.1 EOSINT M270 Xtended machine

An EOSINT M 270 Xtended DMLS machine was used in this PhD thesis work, and it is shown in figure 4.1. The machine is equipped with a 200 W Ytterbium (Yb) continuous fiber laser beam with a wavelength ranging from 1.06 to 1.10  $\mu\text{m}$ . The focused diameter of the Yb laser beam is 0.1 mm. The building volume of the machine is 250 mm x 250 mm x 215 mm [77]. The layer thickness ranges from 20  $\mu\text{m}$  to 40  $\mu\text{m}$ , depending on the material used for fabricating the parts. The 3D CAD model creation, its manipulation, including the support structures generation (the .STL file in output) and the final slicing are done in a separate computer with respect to the machine. Then, the sliced files are imported to the process on-board computer of the machine. It controls the machine and is used for interacting with the user. The process chamber of the machine is located beneath the scanner. The build platform carrier consists of a heating system, which is used for heating up the build platform. The standard operating temperature of the build platform is 35 °C for aluminium, as recommended by the supplier; but it can be raised up to 100 °C. The machine works in Ar gas atmosphere to avoid the oxidation of the material and any problems related to potential explosive environments. Therefore, the building process starts only if concentration of O<sub>2</sub> in the building chamber reaches < 0.1% and during the fabrication process varies from 0.06 to 0.12% during the laser melting. A gas recirculating filter is placed near the machine, this filter extracts the Ar gas from the process chamber, filters it and then supplies it back to the process chamber. The recirculating filter has an external waste gas filter system to purify the waste gas before delivering to the atmosphere. A cooling system is required for extracting the heat in excess developed by the laser during the

process. Compressed air is used to cool the optics of the system.

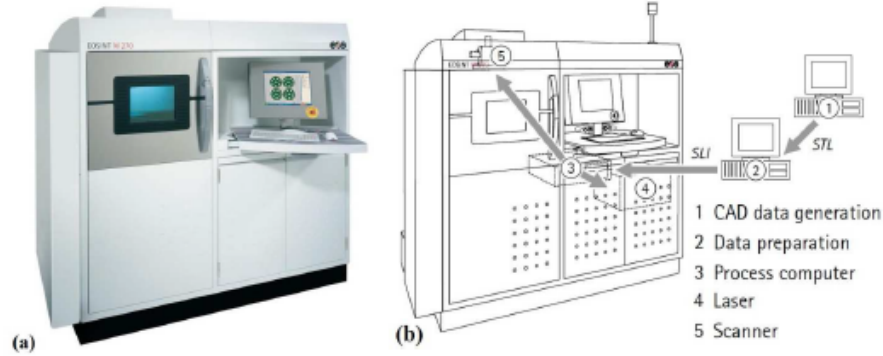


Figure 4.1: Illustration of EOSINT M270 Xtended system [77]

From a practical point of view, this DMLS machine consists of three platforms. They are collector platform, build platform and dispenser platform. Considering the process, the metal powder is initially sieved and charged to the dispenser platform, before the laser sintering process is started. Then the dispenser platform moves up of about  $30\text{ }\mu\text{m}$  to deposit the metal powder on the build platform. Hence the laser beam is passed through the galvanometers, and it melts the region of powder according to the sliced data of 3D CAD geometry. This region solidifies rapidly. The surrounding metal powder is left loose and can be used again after a necessary resieving step (up to 95% of the unused powders could be resieved and recollected). Then the build platform moves to the height of one layer thickness in the downward direction, the recoater deposits another layer of powder on it, and it the laser beam scans the zone based on the sliced file. Therefore the build process is continued until the production of the part is completely finished. Metal powder in excess is stored in the collector platform.

In general, in DMLS technology, you refer to the scanning strategy as the method of raster scanning of the powder bed by the laser beam. Its choice should aim to increase the productivity and the quality level of the fabricated parts: for example free from distortions, warps and porosity. A strategy generally consists of two different phases, one successive to the other during the process: contouring, then fill scanning. The latter one is used to scan all the inner areas of each cross section, whereas contouring is used to perform scanning at their boundaries.

An example is shown in figure 4.2, where fill scan consists of parallel lines and contour scan is done by scanning once at boundaries. The first diagram of figure 4.2 shows parallel scan in one direction, while the second diagram shows the parallel alternate scan.

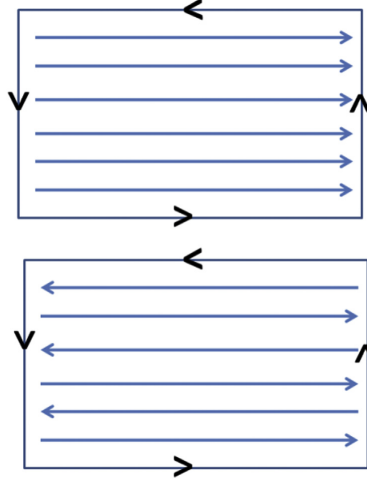


Figure 4.2: Parallel-line scan mode in one direction and in alternate directions

Many scanning options are provided in commercial DMLS machines, which include skywriting and hatch patterns for different requirements.

Four choices for hatch patterns selection are generally available, i.e. along x, along y, both in xy or alternating in xy as shown in figure 4.3. Scanning could be done either along x or along y - figure 4.3(a) and 4.3 (b). If both in x and y options are selected then there will be double exposure on each layer, once along x and the second one along y - figure 4.3 (c). In alternating xy strategy, direction of scanning is changed by  $90^\circ$  for subsequent layers - figure 4.3 (d). Figure 4.3 (e) shows the direction of scanning rotated by  $67^\circ$  between consecutive layers. This is the default value of the hatch pattern in M270 machine for Al alloys, since it is proved to be the optimum to obtain dense parts. However, scanning in lines produces shrinkage stresses, which could be detrimental.

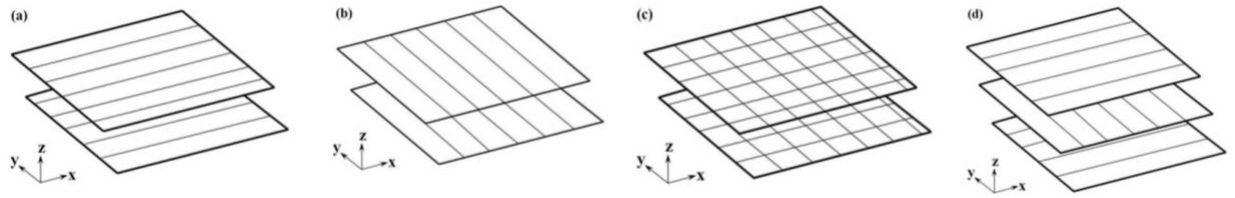


Figure 4.3: Different building hatch patterns for DMLS process [3]

Machines should be used in such a way that the parts having various degrees of complexity could be built efficiently and economically. This is done by choosing the right building orientation of the parts and sacrificial support structures. The part should be oriented in such a way that the minimum number of



layers would be required to build the part. This helps to decrease the time of fabrication and maintains uniform heat buildup. In fact, in DMLS machines, a heating system is set below the base plate (substrate). If the part is built in a “non preferred” orientation, some section of the part would be far away from the heater and it would be difficult for the heater to maintain uniform temperature all along the built.

For a complex part, presenting many overhangs in various angles, orientation of the part would minimize the problems but in some cases would not be able to solve them completely. In those cases, orientation combined with optimization of processing parameters could solve the problem. In order to fabricate parts in some built orientation, support structures are required. The role of a support structure is to prevent the built from falling and displacing. In addition, it helps to dissipate the heat in excess developed in the part during the process.

In principle, the surrounding loose powders act as a support, but for some complex cases containing large surfaces, for example of V or U shape, support structures are required. Support structures have to be removed after the fabrication of the parts, so they should be designed both sufficiently strong to sustain the part and sufficiently “porous” to be detached easily. Their contact area with the part should be minimal to reduce post-processing. So the processing parameters for fabricating supports are different from those for fabricating the parts. In some cases, weak support structures are sufficient: they safeguard the main part from wear and tear during the removal from the substrate. In order to successfully build up thin features, a sacrificial structure is required to avoid their collapsing.

In general, a part does not require the same mechanical properties at all sections. Accordingly, it would be very useful to explain the skin/core strategy which is available in DMLS systems. For example, the outer surface could be required to be hard and wear resistant, while the inner core can be supposed to provide toughness. This requirement is translated into different process parameter settings for outer layers and inner layers, as reported the scheme of figure 4.4. In the above cited example, the process parameters for outer layers should provide high energy, whereas for inner layers provide relatively lower energy. Adopting this strategy accelerates the production. As reported in literature, DirectSteel supplied by EOS is processed by this strategy [77].

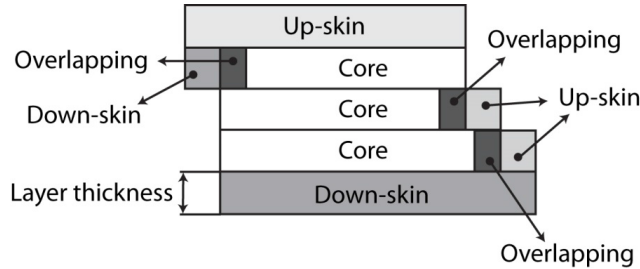


Figure 4.4: Upskin, downskin and core regions [3]

## 4.2 Characterization methods

### 4.2.1 Density and porosity evaluation methods

In the field of porosity measurements, it is better to define some quantities, in order not to generate misunderstandings. Porosity of a part is generally distinguished between:

- total porosity;
- open porosity;
- closed porosity.

Open porosity is the fraction of pores that are accessible from the exterior of the considered body. It can be defined as:

$$P_{open} = \frac{V_{openpores}}{V_{filled} + V_{openpores} + V_{closedpores}} \quad (4.1)$$

On the opposite, closed porosity is the fraction of pores which is not accessible from the exterior of the considered body:

$$P_{closed} = \frac{V_{closedpores}}{V_{filled} + V_{openpores} + V_{closedpores}} \quad (4.2)$$

Total porosity is then the sum of the two previous contributes.

However, these relationships are not so useful when porosity is to be calculated, since density measurements are used. In fact it is possible to define:

- bulk (or geometrical) density;
- apparent density;
- theoretical density.

Theoretical density is defined as:

$$\rho_{theor} = \frac{m_{air}}{V_{filled}} \quad (4.3)$$

where  $m_{air}$  is the mass of the body in air, and  $V_{filled}$  is its volume.

Instead apparent density and bulk density are given by:

$$\rho_{app} = \frac{m_{air}}{V_{filled} + V_{closedpores}} \quad (4.4)$$

$$\rho_{bulk} = \frac{m_{air}}{V_{filled} + V_{closedpores} + V_{openpores}} \quad (4.5)$$

Therefore porosities and densities can be easily correlated as follows:

$$P_{open} = \frac{\rho_{app} - \rho_{bulk}}{\rho_{app}} \quad (4.6)$$

$$P_{closed} = \rho_{bulk} \left( \frac{1}{\rho_{app}} - \frac{1}{\rho_{theor}} \right) \quad (4.7)$$

So, porosity can be estimated by density measurements. Apparent density can be measured using the so-called Archimedes balance equipment, while bulk density either by geometrical means or by the coupling of two weighing, one of the dry sample and one of the sample with its porosity filled by a liquid of known density (in this case apparent density must be prior known). Finally the theoretical density can be estimated by literature and can be measured by picnometry.

Archimede balance, or hydrostatic balance, is based on the Archimede principle. In order to measure apparent density a body is weighted dry and then immersed in a fluid of known density that will penetrate the open porosity of the body. A balance equipped with a specific density measurement device for solid materials was used in this work. Figure 4.5 shows a schematic of the Archimedes measuring principle, indicating the mass evaluation in air and in the fluid (in this thesis work distilled water was used). The used balance has a measuring accuracy of  $\pm 0.1$  mg.

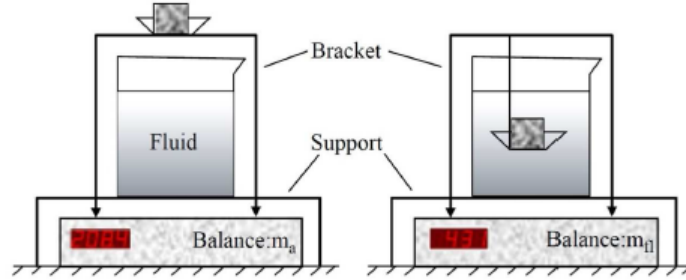


Figure 4.5: Archimedes method scheme [93]

By applying the Archimedes principle, you can obtain this relationship:

$$\rho_{app} = \frac{\rho_{fl} m_{air}}{m_{air} - m_{fl}} \quad (4.8)$$

If not measured by geometrical means (because of the fact that the specimens have not a regular shape), a possible method for the calculation of bulk density is the following: a body is immersed into a liquid which wet its surfaces, and let in the liquid for a sufficiently long time, so that its open pores are completely filled. Then the body is weighted, with the liquid yet inside the pores. The value obtained is:

$$\rho_{bulk} = \frac{m_{air} \rho_{fl}}{m_{dried} - m_{fl}} \quad (4.9)$$

Concerning the picnometry, the method is used to calculate the theoretical density of powders; it is important to have very fine powders, without any closed porosity. To make a picnometry measurement there is need to make four weighing, to know:

- weight of the empty picnometre;
- weight of the picnometre filled with a fluid of known density;
- weight of the picnometre with the powder inside;
- weight of the picnometre with the powder inside, filled with the fluid.

The measurement is not as easy as it seems, since some experimental problems are present: fluid evaporation, thermal fluctuations, not perfect grinding of the powder. In the case of metallic composite powders, for instance, due to the presence of the metallic phase, the grinding of the powder was often not effective, and so data were not precise.

From each process parameter set, it is worth to evaluate porosity by microscopy means. To do this, each sample was cut twice in order to prepare two cross sections of layers lying parallel (index p) and vertical (index v) to the scan plane of the DMLS process, as shown in figure 4.6.

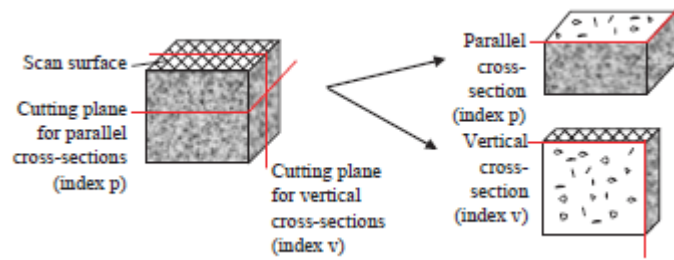


Figure 4.6: Cutting of the test specimen for porosity evaluation showing the two main directions [93]

The section pieces were then grinded, sanded with abrasive paper (granulation from 80 and 4000) and polished using a diamond (up to 1  $\mu\text{m}$ ) paste. The specimens were observed without etching. In each cross section and using 50x magnification on the optical microscope, micrographs were taken at randomly selected positions. In this way it is possible to take several micrographs in which the pores are darker with the respect to the dense regions. The pictures were analysed using the ImageJ-software. A suitable preparation of the black-and-white micrographs is fundamental: selecting the right threshold values in the colours tool box, a clear identification of the pores is possible. With porous samples, the pores might be as big that the internal region of the pores are

illuminated, which leads to a falsification of the porosity measurement. In such cases, these pores need to be blackened manually. The correct black content (porosity) of the cross section can be identified using the in built histogram function and the result is a fraction in % of the total

Finally, the pycnometry method is commonly used to calculate the theoretical density of powders; it is important to have a batch of powders without any closed porosity. To realize a pycnometry measurement it is required to do four weighing, to know:

- $w_1$  weight of the empty pycnometer;
- $w_2$  weight of the pycnometer filled with a fluid of known density  $d_f$ ;
- $w_3$  weight of the pycnometer with the powder inside;
- $w_4$  weight of the pycnometer with the powder inside, filled with the fluid.

The resulting weight of the powder is:

$$w_{\text{powder}} = w_3 - w_1$$

The volume of the powder is the difference between the fluid volume used in the phase 2 and that used in the phase 4:

$$V_{\text{powder}} = \frac{(w_2 - w_1) - (w_4 - w_3)}{gd_f}$$

so that the density of the powder is given from:

$$d_{\text{powder}} = \frac{(w_3 - w_1)d_f}{(w_2 - w_1) - (w_4 - w_3)}$$

The measurement is not as easy as it could seem, since some experimental problems have to be taken into account: fluid evaporation, thermal fluctuations, not perfect grinding of the powder. In the case of metal composite powders, for instance, due to the presence of metal, the grinding of the powder results often not effective, and data are not anymore so reliable.

#### 4.2.2 Mechanical characterization

In this PhD work uniaxial longitudinal tests are pursued by using an EasyDur 3MZ - 5000 equipment. It is moreover fundamental to analyse the fracture surfaces after that the specimens got broken. Three point bending tests and Charpy impact tests and were also pursued on the developed materials. IMCE test was used to measure the elastic modulus of the materials.

Hardness is defined as the resistance of the material to the localized plastic deformation due to the effect of the indenter. Many methods to measure the hardness exist. The most used ones are represented by quantitative methods in which the numerical value associated to the hardness is a geometrical measurement of the indent left on the specimen from the indenter which has a standardized weight and geometry/shape.

Hardness tests are after employed to evaluate mechanical properties because:

1. they are non destructive;
2. the hardness value could be correlated to the ultimate strength and elastic modulus.

In the present work microVickers indentation was pursued. A diamond indenter of pyramidal shape is used. The Vickers hardness value is given by a formula which contains  $P$ , which is the applied load value and  $d$  that is the diagonal length of the indent on the polished surface of the tested sample.

#### **4.2.3 Field Emission Scanning Electron Microscope (FE-SEM)**

A field-emission cathode in the electron gun of a Field Emission Scanning Electron Microscope (FESEM) provides narrower probing beams at low as well as high electron energy, resulting in both improved spatial resolution and minimized sample charging and damage, in comparison with a Scanning Electron Microscope (SEM).

FESEM produces clearer, less electrostatically distorted images with spatial resolution down to 1 - 0.5 nm. Small area contamination spots can be examined at electron accelerating voltages compatible with Energy Dispersive X-ray spectroscopy (EDX). Reduced penetration of low kinetic energy electrons probes closer to the immediate material surface. High quality, low voltage images are obtained with negligible electrical charging of samples. (accelerating voltages range from 0.5 to 30 kV).

In this PhD work a Zeiss model was used to characterize the morphology and more in general the quality of the raw powders, as well as it is required to analyse both the submicrometric details of the DMLS microstructures and the fracture surfaces of the specimens after tensile tests and Charpy impact tests.

#### **4.2.4 X-ray diffraction (XRD)**

X-ray diffraction is a widely used technique for the characterization of the crystalline materials. It is fundamentally based on the capability of atoms to act as scattering centers. When the X-ray radiation interacts with the material, due to the fact the interatomic distances are comparable with the X-ray wavelength, a signal is generated. The Bragg's law is followed:

$$n\lambda = 2d_{hkl}\sin\Theta$$

where  $n$  is an integer,  $\lambda$  the wavelength,  $d_{hkl}$  the interplanar distance of the  $hkl$  planes and angle  $\Theta$  between the incident radiation and the scattering planes. When this equation is satisfied, scattering can occur. In the diffractograms, are shown the peaks intensities as a function of the diffraction angle. Peak position is related to the interplanar distances so that it can be used for the identification of the crystalline present phases.

In this work a diffractometer . This equipment presents a Bragg-Brentano geometry and a  $\text{Cu K}\alpha$  radiation.

#### 4.2.5 Nanohardness and Scanning Probe Microscopy (SPM)

As described before, many methods exist for the determination of metallic materials properties at the micrometric scale, in particular in terms of their mechanical responses. However, concerning nanostructured materials, they become less reliable. Other methods exist to characterize materials with nano or sub-micrometric structures, as the ones obtained after DMLS process.

In particular, a technique known as nanoindentation was quite recently developed to solve some of these issues. Nanoindentation is based on a material resistance to permanent plastic deformation, in terms of its physical working principle. This technique consists in pressing an extremely sharp, hard tip into a surface, under a certain, predetermined load. Through the examination of the tip load and displacement data, the material hardness and reduced elastic modulus can be calculated [93].

The differences between this test and a microtest (for example Vickers) are that the tip geometry and loads are much smaller, and the corresponding indentations/penetrations depths are in the nanometer scale.

Nanoindentations were carried out with an Hysitron instrument (TI 950 TriboIndenter) present at IIT@PoliTo. The equipment is showed in figure 4.7.

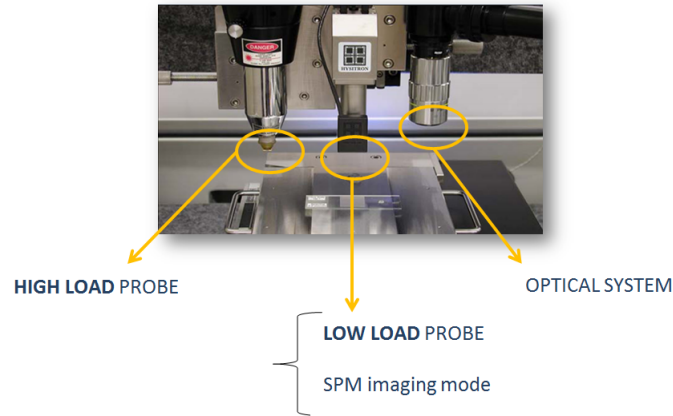


Figure 4.7: Hysitron TI 950 TriboIndenter

This system is made of 3 parts: a low-load testing module, the OmniProbe module and an optical system. A Berkovich tip is mounted in the low-load module, and it consists of a 3 - sided pyramid with an included angle of  $142.3^\circ$ , where the angle from the normal to a face is  $65.35^\circ$ , as reported in the FESEM pictures of figure 4.8.



Figure 4.8: Berkovich tip FESEM images: on the left, tip plus support; on the right, magnification of the tip

In figure 4.9 some examples of the typical load-displacement curves of this technique are reported. These curves are the output of the software which controls the nanoindentation equipment, and in this example they are the results of a series of nanoindentations performed on a fused quartz calibration sample.



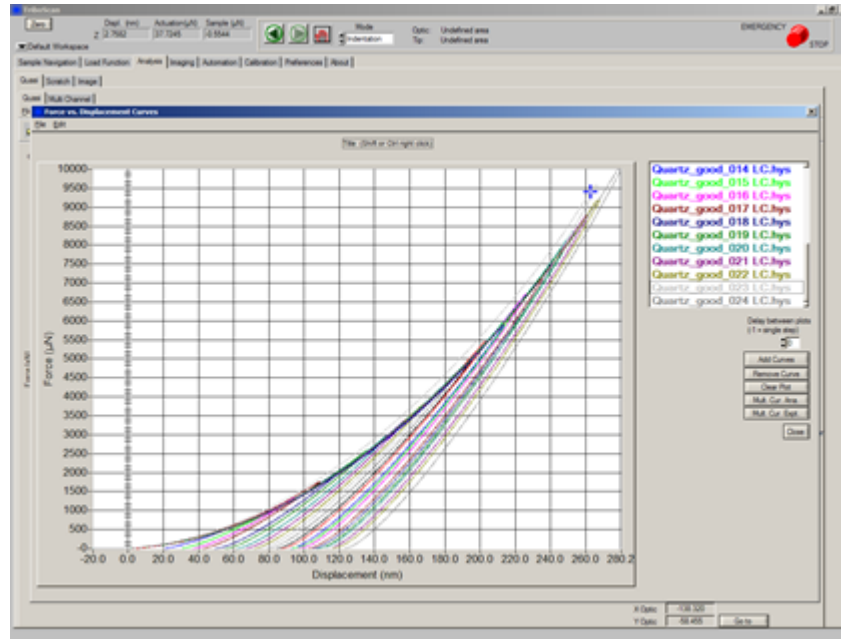


Figure 4.9: Examples of load-displacement curves obtained on a calibration sample

Concerning experimental cases, in which the material is not completely full-filling the requirements about flatness of the indented surface and planarity of the tested sample, the curves would not be as much as overlapping one on the other as in the calibration cases. In order to better understand what a map should consist of, an example of that is reported in figure 4.10: the sample was an aluminium polished one fabricated by DMLS.

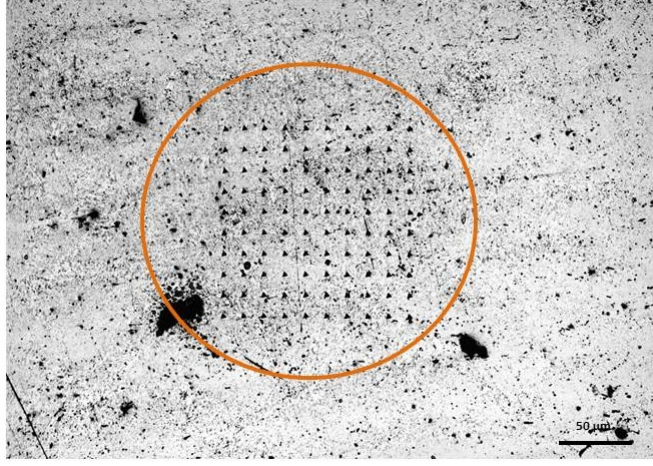


Figure 4.10: Map of indentations on DMLS aluminium sample characterized in this thesis

Hardness and Young's modulus could then be calculated using the Oliver and Pharr Methods based on the unloading curve, as described below.

Oliver and Pharr [94] analysed the load-displacement data and developed equations for calculating hardness ( $H$ ) and reduced elastic modulus ( $E_r$ ), using:

$$E_r = 2S\sqrt{\frac{\pi}{A}} \text{ and } H = \frac{P_{max}}{A}$$

where the tip contact area,  $A$ , is a function of the contact depth derived from the tip area calibration equation, whereas  $S$  and  $P_{max}$  are constants defined prior reduced elastic modulus  $E_r$  is given by:

$$\frac{1}{E_r} = \frac{1 - \nu^2}{E} + \frac{1 - \nu_i^2}{E_i} \quad (4.10)$$

where  $E$  and  $\nu$  are the Young's modulus and Poisson's ratio of the specimen, while  $E_i$  and  $\nu_i$  are material constants for the indenter tip. This equation assumes that the deflection of the tip is zero, which is a reasonable assumption since the diamond tip is extremely rigid, with  $E_i = 1,140$  GPa and  $\nu_i = 0.07$ , respectively.

Traditional Scanning Probe Microscopy (SPM) imaging consists of a sharp tip being forced across a surface while recording interactions between the tip and the sample. The most common SPM technique is the Atomic Force Microscopy (AFM). It employs a scanning technique to produce high-resolution images of a sample's surface by using a cantilever beam that either slides against the surface, being such technique defined as "contact mode", or freely vibrates at a harmonic frequency and intermittently contacts the surface, being such technique termed as "tapping mode". The surface is mapped by using repeated

line scans and monitoring the signal from a laser that is deflected off the cantilever onto a photodiode. This technique can be used to investigate surfaces of both conductors and insulators with very high resolution. The Hysitron TI 950 Tribometer has in-situ SPM imaging capability. In this case the indenter tip is used as probe to raster scan the surface. This provides a lower resolution if compared to an optimized AFM. Nevertheless, a good image quality can be achieved. The Hysitron transducer is a three-plate capacitive device. The tip (Berkovich tip shown in figure 4.8) is screwed into the pickup electrode on the center plate in the structure which is suspended with four Be-Cu springs. The outer two electrodes are fixed in space and driven with an AC signal  $180^\circ$  out of phase with one another. This sets up an electric field potential between the plates that is zero in the center and the magnitude of the signal at either of the plates. A force is applied to the center plate and the tip by applying a large DC offset to the bottom or top plate. This creates an electrostatic attraction that can be calibrated to a force. The theoretical resolution of the instrument is 1.0 nN and 0.04 nm while the maximum applied load is 10 mN. The transducer essentially replaces the AFM cantilever beam and laser combination.

Since displacement or force can be recorded by the transducer, the sample can be scanned with the same piezo-stack that is used for AFM measurements. While scanning as an AFM in contact mode, the transducer is set to maintain a certain contact force between the tip and sample.